Meccanica (2011) 46:625–649
DOI 10.1007/s11012-010-9327-7

ORIGINAL ARTICLE

A time-domain nonlinear system identification method based on multiscale dynamic partitions

Young S. Lee · Stylianos Tsakirtzis · Alexander F. Vakakis · Lawrence A. Bergman · D. Michael McFarland

Received: 29 July 2009 / Accepted: 8 June 2010 / Published online: 4 August 2010

Abstract Based on a theoretical foundation for empirical mode decomposition, which dictates the correspondence between the analytical and empirical slow-flow analyses, we develop a time-domain nonlinear system identification (NSI) technique. This NSI method is based on multiscale dynamic partitions and direct analysis of measured time series, and makes no presumptions regarding the type and strength of the system nonlinearity. Hence, the method is expected to be applicable to broad classes of applications involving time-variant/time-invariant, linear/nonlinear, and smooth/non-smooth dynamical systems. The method leads to nonparametric reduced order models of simple form; *i.e.*, in the form of coupled or uncoupled oscillators with time-varying or time-invariant coefficients forced by nonhomogeneous terms representing nonlinear modal interactions. Key to our method is a slow/fast partition of transient dynamics which leads to the identification of the basic fast frequencies of the dynamics, and the subsequent development of slow-flow models governing the essential dynamics of the system. We provide examples of application of the NSI method by analyzing strongly nonlinear modal interactions in two dynamical systems with essentially nonlinear attachments.

Keywords Slow flow model · Complexification-averaging technique · Empirical mode decomposition · Intrinsic mode function · Nonlinear system identification · Intrinsic modal oscillator

This work was supported in part by the US Air Force Office of Scientific Research through Grant Number FA9550-07-1-0335.

Y.S. Lee (✉)
Mechanical and Aerospace Engineering, New Mexico State University, PO Box 30001, MSC 3450, Las Cruces, NM 88003, USA
e-mail: younglee@nmsu.edu

S. Tsakirtzis
School of Applied Mathematical and Physical Sciences, National Technical University of Athens, P.O. Box 64042, Zografos, Athens 157 10, Greece
e-mail: tsakstel@central.ntua.gr

A.F. Vakakis
Department of Mechanical Science and Engineering, University of Illinois at Urbana-Champaign, 1206 W. Green St., Urbana, IL 61801, USA
e-mail: avakakis@illinois.edu

L.A. Bergman · D.M. McFarland
Department of Aerospace Engineering, University of Illinois at Urbana-Champaign, 104 S., Wright St., Urbana, IL 61801, USA

L.A. Bergman
e-mail: lbergman@illinois.edu

D.M. McFarland
e-mail: dmmcf@illinois.edu

1 Introduction

System identification (SI) in structural dynamics problems usually refers to determining the properties of

a system (through the application of signal processing techniques) by direct analysis of numerical or experimental output and, perhaps, input data. In linear systems this is performed by modal analysis employing techniques such as curve fitting of frequency response functions in the complex plane [1], the Ibrahim time domain method [2], the eigensystem realization algorithm [3], the stochastic subspace identification method [4], and others. Nonlinear SI techniques are often classified as time- or frequency-domain methods; a recent survey of current methods of nonlinear SI was carried out in Kerschen et al. [5].

An important classification of nonlinear SI methods concerns the presumptions made regarding the specific characteristics of the mathematical model of the measured dynamics; in that sense we distinguish between parametric and nonparametric methods. In a parametric method, a particular model is assumed for the dynamical system to be identified, and the aim is to determine the parameters of that model. On the other hand, nonparametric identification makes no presumptions regarding the model of the dynamics to be identified, focusing, for example, on optimal 'functional' representation of a system based on input-output mappings [6]. Hence, an important feature in nonparametric SI analysis is that *there are no a priori assumptions made about the physical model governing the dynamics to be identified*.

Typical nonparametric SI methods include derivation of a reduced-order model (ROM) through proper orthogonal decomposition (POD), Volterra theory, or artificial neural networks. For example, Silva [6] performed nonlinear SI using Volterra theory on aeroelastic systems, developed computationally-efficient ROMs employing an Euler/Navier-Stokes fluid solver, and finally derived analytically Volterra kernels for nonlinear aeroelastic systems from data of flight flutter tests of an active aeroelastic wing aircraft.

There are alternative well-established methods for nonlinear parameter estimation, such as the restoring force surface (RFS) method [7], NARMAX (Nonlinear Auto-Regressive Moving Average models with eXogenous inputs) [8, 9], methods based on Hilbert transforms (FREEVIB and FORCEVIB methods [10, 11]), and others. The harmonic balance technique was applied to nonlinear SI. For example, Thothadri et al. [12] extended nonlinear SI based on the principle of harmonic balance to multi-degree-of-freedom (MDOF) fluid-structure interaction systems. The main advantage of the harmonic balance technique is its usefulness to predict bifurcation behavior of a nonlinear system, for which nonparametric methods are not usually well suited; this is performed by exploiting the periodicity in the response of an experimental system, when parametric time-domain methods such as the NARMAX fail [12]. A multi-staged approach for fitting the excitation of a nonlinear system in nonparametric form was developed in Masri et al. [13, 14]. Also, a general 'data-based' approach for developing ROMs of nonlinear MDOF systems was proposed by assuming no information about the system mass [15, 16]. However, none of these are truly efficient nonparametric methods, since they are only applicable to specific classes of dynamical systems; in addition, some type of functional form is always assumed for modeling the system nonlinearity and the main task becomes the determination of the corresponding coefficients.

Given a sufficiently dense set of sensors, measured time series recorded throughout a mechanical or structural system contains all information regarding the dynamics of that system. This observation highlights the importance of developing effective, straightforward, non-parametric system identification and reduced order modeling methods based on direct analysis of measured time series. These methods should be capable of analyzing strongly nonlinear, complex, multi-component systems and be as utilitarian as (the well established) experimental modal analysis for linear systems. This is precisely the focus of our work: the development of a new methodology for performing nonparametric system identification (eventually leading to reduced order modeling) of broad applicability; *e.g.*, applicable to broad classes of time-variant/time-invariant, linear/nonlinear, and smooth/non-smooth dynamical systems. The need for developing such a system identification technique of broad applicability is dictated by the limitations of current system identification techniques which are either applicable only to linear systems or are tailored to special classes of smooth nonlinear systems. The difficulty in developing nonlinear system identification methodologies of broad applicability is due to the well-recognized highly individualistic nature of nonlinear systems, which restricts the unifying (*i.e.*, the common) dynamical features that are amenable to system identification.

This paper is structured as follows. In Sect. 2 we briefly review the correspondence between analytical and empirical slow flows, which provides a solid theoretical foundation for empirical mode decomposition; by slow flows we denote the underlying (governing) dynamics of the system once the (secondary) fast dynamics are averaged out of the problem [17]. The basic elements of the proposed nonlinear system identification method are then developed in Sect. 3. Finally, in Sect. 4 we validate our proposed technique by performing system identification of the dynamics of 1:3 transient resonance capture in a coupled oscillator with essential (nonlinearizable) stiffness nonlinearity, and of the triggering mechanism of aeroelastic instability of a rigid wing in flow. Our proposed technique relies solely on direct time series measurement and post-processing, and leads to nonparametric reduced order models of simple form; *i.e.*, in the form of coupled or uncoupled oscillators with time-varying or time-invariant coefficients forced by nonhomogeneous terms representing nonlinear modal interactions. Key to our method is a slow/fast partition of time series measurements which leads to the identification of the basic fast frequencies of the dynamics (which also govern the dimensionality of the resulting reduced order model), and the development of slow-flow models describing the important (governing) dynamics of the system.

2 Correspondence between analytical and empirical slow-flow analyses: a review

We consider an n-degree-of-freedom (DOF) dynamical system

$$\dot{\mathbf{X}} = \mathbf{f}(\mathbf{X}, t), \quad \mathbf{X} = \{\mathbf{x}^T \ \dot{\mathbf{x}}^T\}^T \in \mathbb{R}^{2n}, \ t \in \mathbb{R} \tag{1}$$

where $\mathbf{x}$ and $\dot{\mathbf{x}}$ are the displacement and velocity vectors, respectively. To establish an analytical slow-flow model for this system, we employ the complexification-averaging (CX-A) technique [18, 19], which is briefly discussed here.

Assume that the dynamics of interest contains N distinct components at frequencies, $\omega_1, \omega_2, \ldots, \omega_N$, so that the response at each degree of freedom of the system can be expressed as the sum of N independent components,

$$x_k(t) = x_k^{(1)}(t) + x_k^{(2)}(t) + \cdots + x_k^{(N)}(t) \tag{2}$$

where $x_k^{(m)}(t)$, $k = 1, 2, \ldots, n$, $m = 1, 2, \ldots, N$, indicates the component of the response of the k^{th} coordinate associated with frequency ω_m, with the ordering $\omega_1 < \omega_2 < \cdots < \omega_N$.

It turns out that even strongly nonlinear dynamical processes can be analyzed by the (analytical) complexification-averaging (CX-A) technique, first introduced by Manevitch [19] (for an extensive discussion of this technique and numerous applications refer to Vakakis et al. [20]). In particular, for each frequency component in (2) we introduce a new complex variable defined by

$$\psi_k^{(m)}(t) = \dot{x}_k^{(m)}(t) + j\omega_m x_k^{(m)}(t) \triangleq \varphi_k^{(m)}(t) e^{j\omega_m t} \tag{3}$$

where $\varphi_k^{(m)}(t) \in \mathbb{C}$, $k = 1, \ldots, n$, and $e^{j\omega_m t}$ represent the 'slow' and 'fast' (complex) components, respectively, of the m^{th} fast frequency component of the response of the k^{th} coordinate. It is clear that the real dependent variables and their time derivatives can be expressed in terms of the new complex variables as,

$$\begin{aligned} x_k^{(m)}(t) &= \frac{1}{2j\omega_m}\left[\psi_k^{(m)}(t) - \psi_k^{(m)*}(t)\right] \\ \dot{x}_k^{(m)}(t) &= \frac{1}{2}\left[\psi_k^{(m)}(t) + \psi_k^{(m)*}(t)\right] \end{aligned} \tag{4}$$

where asterisk $(\,)^*$ denotes complex conjugate.

In the presence of multiple frequency components, the method of multiphase averaging [21] can be utilized to perform fast-slow partitioning of the dynamics. Substituting into (1), and averaging out fast-frequency components other than $e^{j\omega_m t}$, $m = 1, 2, \ldots, N$, we obtain the slow-flow model in the form,

$$\dot{\Phi}_k = \mathbf{F}_k(\Phi_k), \quad \Phi_k \in \mathbb{C}^N \tag{5}$$

where $\Phi_k = \{\varphi_k^{(1)}, \varphi_k^{(2)}, \ldots, \varphi_k^{(N)}\}^T$, $k = 1, 2, \ldots, n$. We note that the dimension N of this slow-flow model may exceed the number of degrees of freedom of the original dynamical system, since the number of fast frequencies is what determines its dimensionality.

Empirical mode decomposition (EMD) is a numerical technique for decomposing a nonstationary and nonlinear time series into a set of intrinsic oscillatory functions (the so-called intrinsic mode functions or IMFs) at different time scales of the dynamics in an

ad hoc manner requiring no *a priori* system information. The IMFs form a complete and almost orthogonal basis for the time series [22].

In order for a function $c(t)$ to be considered an IMF, it must satisfy the following two basic properties: (i) it must possess exactly one zero between any two consecutive local extrema; and (ii) it must have zero local mean. The main loop of the algorithm for extracting the IMFs of a signal $x(t)$ is summarized as follows [22, 23]: (i) identify all extrema of $x(t)$; (ii) perform (spline-) interpolations between minima (maxima), resulting in an envelope $e_{\min}(t)$ ($e_{\max}(t)$); (iii) compute the average $R(t) = [e_{\min}(t) + e_{\max}(t)]/2$ (considered a residual); (iv) extract the detail $c(t) = x(t) - R(t)$; (v) iterate on the residual $R(t)$. In practice, the above procedure is refined by a *sifting* process, and the inner loop that iterates (i)–(iv) on the detail $c(t)$ runs until the average $R(t)$ can be considered zero-mean to some tolerance (*i.e.*, as a stopping criterion). Once achieved, the detail $c(t)$ is regarded as the effective IMF. This procedure will be denoted the standard EMD method (SEMD).

Suppose that the response of the k^{th} DOF of a discrete dynamical system, $x_k(t)$, can be decomposed into N dominant IMFs, resulting in the decomposition

$$x_k(t) \approx c_1^{(k)}(t) + c_2^{(k)}(t) + \cdots + c_N^{(k)}(t) \tag{6}$$

where $c_m^{(k)}(t)$, $k = 1, 2, \ldots, n$, $m = 1, 2, \ldots, N$, indicates the IMF associated with the dominant frequency ω_m. By construction, EMD yields IMFs sequentially from higher- to lower-frequency components, so an *ad hoc* multi-scale decomposition of the dynamics is performed. Moreover, we adopt notation similar to that used for the analytical slow-flow model; that is, the IMF with the larger subscript is the higher-frequency component. This convention will help avoid confusion when considering the equivalence of the analytical and empirical slow flows.

To check the orthogonality of the IMFs used in the decomposition of the signal (6) we compute its square

$$x_k^2(t) \approx \sum_{i=1}^{N} \left[c_i^{(k)}(t)\right]^2 + 2\sum_{m=1}^{N-1}\sum_{l=m+1}^{N} c_l^{(k)}(t)c_m^{(k)}(t) \tag{7}$$

Then, the overall index of orthogonality (IO [22]) for the decomposition (6) is defined by considering the relative magnitudes of the cross terms in the second part of (7)

$$\mathrm{IO}_k \triangleq \sum_{t=0}^{T}\left[\sum_{m=1}^{N-1}\sum_{l=m+1}^{N} c_l^{(k)}(t)c_m^{(k)}(t)/x_k^2(t)\right] \tag{8}$$

If the decomposition yields completely orthogonal IMFs or if the signal is an IMF itself, then the IO should be zero. Moreover, the closer the IO is to zero, the better the orthogonality between the IMFs. The quantification of the degree of orthogonality between IMFs provided by the index (8) paves the way for optimizing the extracted basis of IMFs to ensure minimization of the orthogonality index.

In addition to the issue of resolution of the decomposition, the SEMD method is often incapable of generating a set of 'proper' and/or almost orthogonal IMFs. The SEMD does not provide a unique decomposition of a signal and strongly depends on a free stopping parameter; that is, the decomposition is not robust in practice, particularly when the signal corresponds to a strongly nonlinear transient dynamical process. Furthermore, it fails to extract high-frequency components hidden in a signal containing inflection-like points.

Although improvement methods for EMD performance employ similar principles, in this study we adopt the use of masking signals with the Matlab codes developed by Rilling et al. [23]. To make a distinction from the standard EMD, our suggested enhanced method will be referred to as advanced EMD method (AEMD [17]).

Drawing from the analyticity properties of complex signals, we examine the analyticity of IMFs [24] in order to establish correspondence or equivalence between an (analytical) slow-flow model defined by the complexification-averaging technique and the dominant (proper) IMFs (*i.e.*, the empirical slow flow) derived by EMD analysis. Taking into account the properties of the Hilbert transform, we introduce the following analytic complexification of the m^{th} IMF, $c_m^{(k)}(t)$,

$$\hat{\psi}_k^{(m)}(t) = c_m^{(k)}(t) + j\mathcal{H}[c_m^{(k)}(t)] \triangleq \hat{A}_m^{(k)}(t)e^{j\hat{\theta}_m^{(k)}(t)} \tag{9}$$

which by construction is an analytic signal. The instantaneous envelope and phase of this IMF can then

be computed by

$$\hat{A}_m^{(k)}(t) = \sqrt{c_m^{(k)}(t)^2 + \mathcal{H}[c_m^{(k)}(t)]^2}$$
$$\hat{\theta}_m^{(k)}(t) = \tan^{-1}\left[\mathcal{H}[c_m^{(k)}(t)]/c_m^{(k)}(t)\right] \tag{10}$$

and its instantaneous frequency, by

$$\begin{aligned}\hat{\omega}_m^{(k)}(t) &= \frac{d}{dt}\hat{\theta}_m^{(k)}(t) \\ &= \frac{[c_m^{(k)}(t)\frac{d}{dt}\mathcal{H}[c_m^{(k)}(t)] - \dot{c}_m^{(k)}(t)\mathcal{H}[c_m^{(k)}(t)]]}{c_m^{(k)}(t)^2 + \mathcal{H}[c_m^{(k)}(t)]^2}\end{aligned} \tag{11}$$

It follows that the analytic signal (9) can be partitioned in terms of slow and fast components according to the expression,

$$\hat{\psi}_k^{(m)}(t) = \hat{A}_m^{(k)}(t)e^{j[\hat{\theta}_m^{(k)}(t)-\omega_m t]}e^{j\omega_m t} \tag{12}$$

which is in a form similar to the analytical slow flow, although no *a priori* slow-fast partition of the dynamics was assumed when decomposing the IMF. Recognizing $e^{j\omega_m t}$ as the fast component of the dynamics of the IMF, we conclude that the remaining partition $\hat{A}_m^{(k)}(t)e^{j[\hat{\theta}_m^{(k)}(t)-\omega_m t]}$ plays the role of the slow component of its dynamics. Clearly, for such a slow/fast partition of the IMF to hold, the instantaneous amplitude, phase and frequency of the IMF must be slowly varying compared to the corresponding fast frequency ω_m of the IMF. This is an assumption that will be made throughout this study, in order for the results of EMD to conform with the following theoretical developments.

Now, we consider an alternative complexification of the m^{th} IMF $c_m^{(k)}(t)$ in the form

$$\hat{\hat{\psi}}_k^{(m)}(t) = \dot{c}_m^{(k)}(t) + j\omega_m c_m^{(k)}(t) \triangleq \hat{\hat{A}}_m^{(k)}(t)e^{j\hat{\hat{\theta}}_m^{(k)}(t)} \tag{13}$$

which bears similarity to the complexification (3). If the complex function $\hat{\hat{\psi}}_k^{(m)}(t)$ is analytic, then so is the function $j\hat{\hat{\psi}}_k^{(m)}(t) = -\omega_m c_m^{(k)}(t) + j\dot{c}_m^{(k)}(t)$. This implies that its imaginary part is the Hilbert transform of its real part,

$$\dot{c}_m^{(k)}(t) = -\omega_m \mathcal{H}[c_m^{(k)}(t)] \tag{14}$$

Furthermore, if condition (14) is satisfied, then there should be an equivalence between the analytical slow flow defined by (2) and the analytical empirical slow flow defined by (6). This is because both expressions represent identical decompositions of the time series in terms of slowly modulated fast components at distinct frequencies. It follows that the following expressions of equivalence

$$x_k^{(m)}(t) = c_m^{(k)}(t) \quad \text{and} \quad \dot{x}_k^{(m)}(t) = \dot{c}_m^{(k)}(t) \tag{15}$$

should hold, which implies that $\dot{c}_m^{(k)}(t)$ should correspond to the m^{th} IMF of the velocity signal $\dot{x}_k^{(m)}(t)$. Then, (13) can be rewritten as

$$\begin{aligned}\hat{\hat{\psi}}_k^{(m)}(t) &= \dot{c}_m^{(k)}(t) + j\omega_m c_m^{(k)}(t) \\ &= -\omega_m \mathcal{H}[c_m^{(k)}(t)] + j\omega_m c_m^{(k)}(t) \\ &= j\omega_m\left(c_m^{(k)}(t) + j\mathcal{H}[c_m^{(k)}(t)]\right) \\ &= j\omega_m \hat{\psi}_k^{(m)}(t)\end{aligned} \tag{16}$$

Therefore, the analytic signal $\hat{\psi}_k^{(m)}(t)$ in (9) and the complex function $\hat{\hat{\psi}}_k^{(m)}(t)$ (which is also analytic by (14)) in (13) are equivalent, such that

$$\hat{\psi}_k^{(m)}(t) = \frac{1}{j\omega_m}\hat{\hat{\psi}}_k^{(m)}(t) \equiv \frac{1}{j\omega_m}\psi_k^{(m)}(t) \tag{17}$$

where $\psi_k^{(m)}(t)$ is derived from a mathematical (or analytical) model by the (analytic) complexification in (3), whereas $\hat{\hat{\psi}}_k^{(m)}(t)$ is obtained by the EMD (or AEMD) of the (experimental or numerical) measured time series via (6) and its complexification (13).

Now, we can assert the correspondence between the analytical and empirical slow flows by noting that (17) leads to the equivalence of the slow parts resulting from CX-A analysis and EMD

$$\hat{A}_m^{(k)}(t)e^{j[\hat{\theta}_m^{(k)}(t)-\omega_m t]} \approx \frac{1}{j\omega_m}\varphi_k^{(m)}(t) \tag{18}$$

from which the analytical slow flow can be expressed in terms of the empirical slow flow as

$$\varphi_k^{(m)}(t) \approx j\omega_m \hat{A}_m^{(k)}(t)e^{j[\hat{\theta}_m^{(k)}(t)-\omega_m t]} \tag{19}$$

The equivalence between the analytical and empirical slow flows based on the assumption of analyticity of the IMFs can then be restated as follows. From (3), (4) and (15), we write,

$$\begin{aligned}\hat{\hat{\psi}}_k^{(m)}(t) &= \dot{c}_m^{(k)}(t) + j\omega_m c_m^{(k)}(t) \equiv \psi_k^{(m)}(t)\\ &= \varphi_k^{(m)}(\tau)e^{j\omega_m t}\\ &= |\varphi_k^{(m)}(\tau)|e^{j\theta_k^{(m)}(\tau)}e^{j\omega_m t}\\ &= |\varphi_k^{(m)}(\tau)|e^{j[\omega_m t+\theta_k^{(m)}(\tau)]}\end{aligned} \tag{20}$$

where the slow-time scale τ is introduced to indicate that the complex variable $\varphi_k^{(m)}(\tau)$ is a slowly varying component with respect to the fast-varying part $e^{j\omega_m t}$. In this multiscale formulation the slow temporal variable τ is considered to be independent from the fast temporal variable t [25]. Thus, the slowly varying envelope and phase, $|\varphi_k^{(m)}(\tau)|$ and $\theta_k^{(m)}(\tau)$, should correspond to the corresponding quantities $\omega_m \hat{A}_m^{(k)}(t)$ and $\hat{\theta}_m^{(k)}(t) - \omega_m t$ in (19), respectively.

The empirical slow flow can then be expressed in terms of the real and imaginary parts of $\psi_k^{(m)}(t)$ such that

$$\begin{aligned}c_m^{(k)}(t) &= \frac{1}{\omega_m}\mathrm{Im}[\varphi_k^{(m)}(\tau)e^{j\omega_m t}]\\ &= \frac{1}{\omega_m}|\varphi_k^{(m)}(\tau)|\sin\big[\omega_m t + \theta_k^{(m)}(\tau)\big]\\ \dot{c}_m^{(k)}(t) &= \mathrm{Re}[\varphi_k^{(m)}(\tau)e^{j\omega_m t}]\\ &= |\varphi_k^{(m)}(\tau)|\cos\big[\omega_m t + \theta_k^{(m)}(\tau)\big]\end{aligned} \tag{21}$$

Recalling that $\mathcal{H}[\cos\omega t] = \sin\omega t$ and $\mathcal{H}[\sin\omega t] = -\cos\omega t$, we derive

$$\begin{aligned}\mathcal{H}[c_m^{(k)}(t)] &= \frac{1}{\omega_m}\mathcal{H}\big[|\varphi_k^{(m)}(\tau)|\sin[\omega_m t + \theta_k^{(m)}(\tau)]\big]\\ &= \frac{1}{\omega_m}|\varphi_k^{(m)}(\tau)|\mathcal{H}\big[\sin[\omega_m t + \theta_k^{(m)}(\tau)]\big]\\ &= -\frac{1}{\omega_m}|\varphi_k^{(m)}(\tau)|\cos[\omega_m t + \theta_k^{(m)}(\tau)]\\ &= -\frac{1}{\omega_m}|\varphi_k^{(m)}(\tau)|\cos[\omega_m t + \theta_k^{(m)}(\tau)]\\ &= -\frac{1}{\omega_m}\dot{c}_m^{(k)}(t)\end{aligned} \tag{22}$$

where Hilbert transformation is carried out only with respect to the fast time scale. This verifies the condition (14) for the analytic equivalence between the slow flow and dominant IMFs. Even without introducing the slow time scale in (20), one can derive the analyticity condition (22) by means of the Bedrosian Theorem [26] based on the analyticity of the slow flow $\varphi_k^{(m)}(t)$ with the notation of the fast time scale retained.

Again, we emphasize that we applied the Hilbert transformation only with respect to the fast time scale in (22), ignoring the slow time dependence. That is, if a function behaves as a simple harmonic function, $c(t) = Ae^{j\omega t}$ (A constant with respect to time variation), then $\dot{c}(t) = j\omega Ae^{j\omega t} = j\omega c(t)$. Hilbert transformation of the harmonic function yields $\mathcal{H}[c(t)] = -je^{j\omega t} = -jc(t)$ so that $\mathcal{H}[[\mathcal{H}[c(t)]] = -c(t)$. This leads to the relations $\dot{c}(t) = -\omega\mathcal{H}[c(t)]$ and $\ddot{c}(t) = -\omega^2 c(t) \Rightarrow \ddot{c}(t) + \omega^2 c(t) = 0$. This last expression obviously represents a harmonic oscillator, and can be applied to proper IMFs. That is, we write

$$\ddot{c}_m^{(k)}(t) + \omega_m^2 c_m^{(k)}(t) = 0 \tag{23}$$

Moreover, as discussed in Lee et al. [17], the assumed slow/fast partition of the IMFs and the assumption of harmonic dependence with respect to the fast time scale imply the analyticity condition (14) for these IMFs.

The derivations in this section show that we can associate the EMD results with the underlying slow-flow dynamics, a result which provides a physics-based foundation for EMD. In particular, we showed that if the analyticity condition (14) is satisfied, then proper IMFs can be associated with components of the slow dynamics of corresponding frequencies. In summary, by associating the EMD results to the slow-flow dynamics of a dynamical system we demonstrate that the IMFs provide significant physical insight to the dynamics, a feature that will be employed in this work. Some demonstrative examples that highlight the correspondence between the EMD results and slow flows are given in Lee et al. [17].

3 Time-domain nonlinear system identification (NSI)

Consider a times series generated (computationally or experimentally) from the response of the n-degree-of-freedom (DOF) dynamical system (1). Assume that the governing dynamics contains N distinct components at ('fast') frequencies, $\omega_1, \omega_2, \ldots, \omega_N$, so that the response of each degree of freedom, $x_k(t)$, $k = 1, 2, \ldots, n$, can be expressed as the sum of N independent 'slowly' modulated harmonic components.

Then, based on the equivalence between analytical and empirical slow-flow analyses discussed in Lee et al. [17] and summarized in the previous section, it is reasonable to define the following one-to-one correspondence between the representations of the time series in terms of the CX-A method and numerical EMD

$$\begin{aligned}\text{CX-A}: x_k(t) &\approx x_k^{(1)}(t) + \cdots + x_k^{(m)}(t) \\ &\quad + \cdots + x_k^{(N)}(t) \\ \Longleftrightarrow \quad \text{EMD}: x_k(t) &\approx c_1^{(k)}(t) + \cdots + c_m^{(k)}(t) \\ &\quad + \cdots + c_N^{(k)}(t)\end{aligned} \tag{24}$$

where $m = 1, 2, \ldots, N$, indicates the component of the response of the k^{th} coordinate (DOF) associated with frequency ω_m, with the ordering $\omega_1 < \omega_2 < \cdots < \omega_N$, and $k = 1, 2, \ldots, n$. Note that the correspondence (24) maintains its physical meaning if the frequency components represent dominant and not spurious harmonics of the response [17].

Based on the correspondence (24) between the analytical and empirical slow-flow analyses, we perform nonlinear system identification (NSI) which will lead to a reduced-order model (ROM) or, more generally, to a *nonlinear interaction model (NIM)* in terms of *intrinsic modal oscillators (IMOs)*. We define IMOs as *the equivalent linear oscillators that can reproduce a given time series over different time scales*. For proper empirical slow-flow decompositions [17], IMOs are typically expressed as a set of linear, damped oscillators having as forcing functions nonlinear modal interactions. A basic requirement is that each IMO should approximately reproduce the corresponding dominant IMF, provided that the fast frequencies of the time series are well-separated (distinct).

It follows that, in order to perform NSI analysis of the dynamics corresponding to $x_k(t)$, we should define an IMO corresponding to (*i.e.*, reproducing) the m^{th} component of the k^{th} DOF response in the form

$$\begin{aligned}&\ddot{x}_k^{(m)}(t) + 2\zeta_k^{(m)}\omega_m \dot{x}_k^{(m)}(t) + \omega_m^2 x_k^{(m)}(t) \\ &\quad = F_k^{(m)}(t)\end{aligned} \tag{25}$$

where the coefficients $\zeta_k^{(m)}$ and ω_m are assumed to be constant, and the nonhomogeneous term $F_k^{(m)}(t)$ represents a time-dependent forcing term describing the nonlinear modal interaction of the m^{th} component of the k^{th} DOF with the other components of the dynamics. In principle, this nonhomogeneous term can be expressed in terms of slow-fast partitions of all participating frequency components; that is, we can write

$$\begin{aligned}F_k^{(m)}(t) = \text{Re}\big[&\Lambda_k^{(1)}(t)e^{j\omega_1 t} + \Lambda_k^{(2)}(t)e^{j\omega_2 t} + \cdots \\ &+ \Lambda_k^{(m)}(t)e^{j\omega_m t} + \cdots + \Lambda_k^{(N)}(t)e^{j\omega_N t}\big]\end{aligned} \tag{26}$$

where Re[·] represents the real part. However, because of the linear structure of the IMO, it should be clear that the only term that can produce an $\mathcal{O}(1)$ dynamic response is the one with fast frequency ω_m (*i.e.*, the eigenfrequency of the IMO). Hence, it is justified to approximately express the IMO in the simplified form

$$\begin{aligned}&\ddot{x}_k^{(m)}(t) + 2\zeta_k^{(m)}\omega_m \dot{x}_k^{(m)}(t) + \omega_m^2 x_k^{(m)}(t) \\ &\quad \approx \text{Re}[\Lambda_k^{(m)}(t)e^{j\omega_m t}] = \frac{1}{2}\big(\Lambda_k^{(m)}(t)e^{j\omega_m t} + \text{cc}\big)\end{aligned} \tag{27}$$

where $\Lambda_k^{(m)}(t)$ ($e^{j\omega_m t}$) represents the slow (fast) component of the dominant nonlinear modal interaction, and 'cc' denotes complex conjugate.

We make a remark at this point regarding the time invariance of the eigenfrequency and damping of the IMO in (27). This time invariance is dictated by the temporal evolution of the corresponding dominant harmonic of the time series at frequency ω_m (which can be numerically checked by studying the wavelet spectrum of the time series $x_k(t)$ [17]). In cases of (slow) time variation of the dominant frequency of a component in the time series representation (24), it will be necessary to introduce a time-varying IMO to represent the corresponding dynamics, but this will not destroy the linear structure of (27). Hence, time variance or invariance of the IMOs is determined by the temporal evolutions of the corresponding frequency components of the time series. In this work we will only be concerned with time invariant IMOs and leave the issue of time variance of IMOs for future work.

The issue now is to identify the modal parameters of the IMO (27) and, more importantly, its forcing term representing the nonlinear modal interaction. To this end, we apply CX-A analysis by introducing the new complex variable

$$\psi_k^{(m)}(t) = \dot{x}_k^{(m)}(t) + j\omega_m x_k^{(m)}(t) \triangleq \varphi_k^{(m)}(t)e^{j\omega_m t} \tag{28}$$

which, when substituted into (27), yields the complexification of the IMO

$$
\begin{aligned}
&\big[\dot{\varphi}_k^{(m)} + j\omega_m \varphi_k^{(m)}\big] e^{j\omega_m t} \\
&\quad - \frac{j\omega_m}{2}\big[\varphi_k^{(m)} e^{j\omega_m t} + \varphi_k^{(m)^*} e^{-j\omega_m t}\big] \\
&\quad + 2\zeta_k^{(m)}\omega_m \frac{1}{2}\big(\varphi_k^{(m)} e^{j\omega_m t} + \varphi_k^{(m)^*} e^{-j\omega_m t}\big) \\
&\quad + \frac{\omega_m^2}{2j\omega_m}\big(\varphi_k^{(m)} e^{j\omega_m t} - \varphi_k^{(m)^*} e^{-j\omega_m t}\big) \\
&\approx \frac{1}{2}\big(\Lambda_k^{(m)}(t) e^{j\omega_m t} + \Lambda_k^{(m)^*}(t) e^{-j\omega_m t}\big) \qquad (29)
\end{aligned}
$$

Multiplying both sides of (29) by $e^{-j\omega_m t}$ and averaging out fast terms other than $e^{j\omega_m t}$, we obtain a relation between the forcing amplitude of the nonlinear modal interaction and the complex amplitude of the analytical slow flow

$$
\Lambda_k^{(m)}(t) \approx 2\big[\dot{\varphi}_k^{(m)}(t) + \zeta_k^{(m)}\omega_m \varphi_k^{(m)}(t)\big] \qquad (30)
$$

This result indicates that, when the CX-A model is known, the nonlinear modal interaction $\Lambda_k^{(m)}(t)$ can be determined directly from the analytical slow-flow model via the relation (30). However, when the time series is obtained from an experiment, a slow-flow model does not exist so that an alternative approach needs to be followed. In this case, we invoke the equivalence of the EMD results and the underlying slow flow governing the dynamics in order to approximate the amplitudes $\varphi_k^{(m)}$ in (30) by the slow component of the respective IMF of the experimental time series derived by EMD analysis. That is, we employ the equivalence (19)

$$
\varphi_k^{(m)}(t) \approx j\omega_m \hat{A}_m^{(k)}(t) e^{j\theta_m^{(k)}(t)} \qquad (31)
$$

where the envelope $\hat{A}_m^{(k)}(t)$ and the phase $\theta_m^{(k)}(t) = \hat{\theta}_m^{(k)}(t) - \omega_m t$ are extracted from direct EMD analysis of the time series (*cf.* (9)–(12)). Then, (30) can be rewritten as

$$
\begin{aligned}
\Lambda_k^{(m)}(t) \approx 2\bigg[&\frac{d}{dt}\big(j\omega_m \hat{A}_m^{(k)}(t) e^{j\theta_m^{(k)}(t)}\big) \\
&+ j\zeta_k^{(m)}\omega_m^2 \hat{A}_m^{(k)}(t) e^{j\theta_m^{(k)}(t)}\bigg] \qquad (32)
\end{aligned}
$$

where $k = 1, 2, \ldots, n$, and $m = 1, 2, \ldots, N$. This provides a way for estimating the modal interaction provided that the eigenfrequency and viscous damping ratio of the IMO are known. The eigenfrequency ω_m is directly determined by performing wavelet analysis of the time series and constructing wavelet spectra in time [17]. The viscous damping ratio is determined by an optimization process based on the requirement that the response of the IMO should reproduce the IMF corresponding to the dominant frequency ω_m; hence, the damping factor is determined by minimizing the normalized mean square errors between the envelope of the IMF $c_m^{(k)}(t)$ and the response of the IMO $x_k^{(m)}(t)$.

Therefore, the response of the IMO (27) can be written as

$$
\begin{aligned}
&x_k^{(m)}(t) \\
&\quad = x_{k,h}^{(m)}(t) + x_{k,p}^{(m)}(t) \\
&\quad = e^{-\zeta_k^{(m)}\omega_m t}\big[x_k^{(m)}(0)\cos\omega_{m,d}t \\
&\qquad + \frac{1}{\omega_{m,d}}\big\{\dot{x}_k^{(m)}(0) + \zeta_k^{(m)}\omega_m x_k^{(m)}(0)\big\}\sin\omega_{m,d}t\big] \\
&\qquad + \frac{1}{\omega_{m,d}}\int_0^t e^{-\zeta_k^{(m)}\omega_m(t-s)}\sin\omega_{m,d}(t-s) \\
&\qquad \times \mathrm{Re}[\Lambda_k^{(m)}(s) e^{j\omega_m s}]ds \qquad (33)
\end{aligned}
$$

where the first term $x_{k,h}^{(m)}(t)$ indicates the homogeneous or transient solution, and the second term $x_{k,p}^{(m)}(t)$ implies the particular or steady-state solution; moreover, the initial conditions are matched to the respective initial conditions of the corresponding IMF, $x_k^{(m)}(0) = c_m^{(k)}(0)$, $\dot{x}_k^{(m)}(0) = \dot{c}_m^{(k)}(0)$; and $\omega_{m,d}^2 = \omega_m^2(1 - \zeta_k^{(m)2})$. We note that the solution (33) is valid only for $\zeta_k^{(m)} < 1$ (*i.e.*, for the underdamped case). Similar expressions, however, hold for critically damped or overdamped IMOs.

Since the previous analysis was based on a slow/fast decomposition of the dynamics (*i.e.*, on the assumption that the IMFs and the dominant harmonics of the signal are in the form of slowly-modulated narrowband oscillations), it is necessary that the quantities $\Lambda_k^{(m)}(t)$, $\hat{A}_m^{(k)}(t)$, and $\theta_m^{(k)}(t)$ are slowly-varying terms that depend on a slow time scale denoted by τ (that is, $|\dot{\tau}| \ll 1$). Hence, the expression (32) computes the slow component of the nonlinear modal interaction assuming that the fast component is approximately harmonic (*i.e.*, $e^{j\omega_m t}$). Also, substituting the small time scale τ in (30), we can approximate the forcing ampli-

tude such that

$$\Lambda_k^{(m)}(\tau) \approx 2\left(\frac{d}{dt}\varphi_k^{(m)}(\tau) + \zeta_k^{(m)}\omega_m\varphi_k^{(m)}(\tau)\right) \approx 2\zeta_k^{(m)}\omega_m\varphi_k^{(m)}(\tau) \tag{34}$$

because $|\frac{d}{dt}\varphi_k^{(m)}(\tau)| \ll 1$. If this approximation holds, it can be shown that the particular solution of the IMO equation (27) can be obtained as

$$x_{k,p}^{(m)}(t) \approx c_m^{(k)}(t) \tag{35}$$

which recovers the equivalence (15) between the IMFs and the underlying slow-flow dynamics.

Alternatively but equivalently to (32), we can calculate the nonlinear modal interaction $\Lambda_k^{(m)}(t)$ directly in terms of the IMFs. To this end, rewrite (30) by multiplying both sides by $e^{j\omega_m t}$

$$\frac{1}{2}\Lambda_k^{(m)}(t)e^{j\omega_m t} \approx \big(\dot{\varphi}_k^{(m)}(t) + j\omega_m\varphi_k^{(m)}(t)\big)e^{j\omega_m t} - j\omega_m\varphi_k^{(m)}(t)e^{j\omega_m t} + \zeta_k^{(m)}\omega_m\varphi_k^{(m)}(t)e^{j\omega_m t} \tag{36}$$

Recalling the equivalence between the analytical and empirical slow flows based on (15), we rewrite (21) as

$$\begin{aligned} c_m^{(k)}(t) &= \frac{1}{\omega_m}\mathrm{Im}[\varphi_k^{(m)}(t)e^{j\omega_m t}] \\ \dot{c}_m^{(k)}(t) &= \frac{1}{\omega_m}\mathrm{Im}\big[\big(\dot{\varphi}_k^{(m)}(t) + j\omega_m\varphi_k^{(m)}(t)\big)e^{j\omega_m t}\big] \\ &= \mathrm{Re}[\varphi_k^{(m)}(t)e^{j\omega_m t}] \\ &= -\omega_m\mathcal{H}[c_m^{(k)}(t)] \end{aligned} \tag{37}$$

where the fast time scale t is retained. Then, the imaginary part of (36) can be written as

$$\frac{1}{2\omega_m}\mathrm{Im}[\Lambda_k^{(m)}(t)e^{j\omega_m t}] \approx \dot{c}_m^{(k)}(t) + \zeta_k^{(m)}\omega_m c_m^{(k)}(t) - \mathrm{Im}[j\varphi_k^{(m)}(t)e^{j\omega_m t}] \tag{38}$$

Noting that

$$\mathrm{Im}[j\varphi_k^{(m)}(t)e^{j\omega_m t}] \equiv \mathrm{Re}[\varphi_k^{(m)}(t)e^{j\omega_m t}] \tag{39}$$

and using (37), we can simplify (38) to

$$\mathrm{Im}[\Lambda_k^{(m)}(t)e^{j\omega_m t}] \approx 2\zeta_k^{(m)}\omega_m^2 c_m^{(k)}(t) \tag{40}$$

The real part of the nonlinear modal interaction can then be calculated directly from the approximate expression of the IMO (27) by substituting the equivalence relation between the analytical and empirical slow flows,

$$\begin{aligned} &\mathrm{Re}[\Lambda_k^{(m)}(t)e^{j\omega_m t}] \\ &\quad\approx \ddot{c}_m^{(k)}(t) + 2\zeta_k^{(m)}\omega_m\dot{c}_m^{(k)}(t) + \omega_m^2 c_m^{(k)}(t) \\ &\quad\approx 2\zeta_k^{(m)}\omega_m\dot{c}_m^{(k)}(t) = -2\zeta_k^{(m)}\omega_m^2\mathcal{H}[c_m^{(k)}(t)] \end{aligned} \tag{41}$$

where the condition (23) for analyticity of the IMF and its harmonic dependence are utilized. In fact, although the result (41) is sufficient to compute the response of the IMO (27), we express the forcing amplitude directly in terms of the IMFs to prove that the resulting relation is equivalent to (34). Indeed, combining (40) and (41), we obtain

$$\begin{aligned} &\Lambda_k^{(m)}(t) \\ &\quad= \big\{\mathrm{Re}[\Lambda_k^{(m)}(t)e^{j\omega_m t}] + j\,\mathrm{Im}[\Lambda_k^{(m)}(t)e^{j\omega_m t}]\big\}e^{-j\omega_m t} \\ &\quad\approx 2j\zeta_k^{(m)}\omega_m^2\big[c_m^{(k)}(t) + j\,\mathcal{H}[c_m^{(k)}(t)]\big]e^{-j\omega_m t} \end{aligned} \tag{42}$$

Note that, replacing the analytical slow flow with the corresponding IMF and using the analyticity condition (14), we can rewrite (28) as

$$\begin{aligned} \psi_k^{(m)}(t) &= \dot{c}_m^{(k)}(t) + j\omega_m c_m^{(k)}(t) \\ &= j\omega_m\big\{c_m^{(k)}(t) + j\mathcal{H}[c_m^{(k)}(t)]\big\} \\ &\equiv \varphi_k^{(m)}(t)e^{j\omega_m t} \end{aligned} \tag{43}$$

This simplifies (42) into

$$\Lambda_k^{(m)}(t) \approx 2\zeta_k^{(m)}\omega_m\varphi_k^{(m)}(t) \tag{44}$$

which verifies that the derivation (34) is correct under the assumption of analyticity of the IMF and its harmonic dependence. Note here that the forcing amplitude in (34) or (44) is a simplified approximation to the slowly-varying nonlinear modal interaction, and is valid only when the IMF possesses a perfect harmonic dependence. In practice, the EMD analysis of a time series does not generate IMFs amenable to perfect slow/fast partition and possessing exact harmonic dependence on the fast time scale; hence, the time derivative term in the expression for the nonlinear modal interaction (30) may not always be negligible, in which case implementation of the more complete expression (32) is preferable. Nonetheless, we

will demonstrate that the approximation (34) or (44) is still useful as an alternate and simple way to compute the nonlinear modal interactions between the IMOs.

We emphasize at this point that the basic assumptions for constructing IMOs of the general form (27) are: (i) that their fast frequencies are well-separated; (ii) that the wavelet spectrum of the k^{th} DOF response possesses nearly constant (*i.e.*, narrowband) fast frequency components; and (iii) that it is possible to introduce a slow-fast partition of the dynamics for each fast frequency component. In summary, the IMO modeling the component of the dynamics in the vicinity of frequency ω_m of the k^{th} DOF is in the form of a linear oscillator with a forcing term representing the nonlinear modal interaction of this component with other such components. Such forcing terms provide us with information on the level and the (slow) temporal dependence of nonlinear modal interactions between different harmonic components of the time series. The use of linear models for studying even strongly nonlinear dynamical interactions is enabled by the accurate identification of the dominant frequencies at which these interactions occur, and by the demonstrated equivalence between the IMFs computed by EMD and the underlying slow-flow dynamics [17]. The basis for the aforementioned reduced order modeling procedure is the construction of IMOs that accurately reproduce the dominant IMFs of the measured time series. This is not an *ad hoc* requirement since, as discussed in Lee et al. [17], the slowly varying envelopes and phases of the dominant IMFs of the responses of coupled oscillators coincide with the slow flow of the problem. Hence, the construction of the IMOs is formal; in fact, the equivalence between EMD and slow flow dynamics provides a theoretical underpinning of, and gives physical meaning to, the dominant IMFs [17].

4 Applications of the NSI method

The correspondence between the analytical and empirical slow flows was demonstrated in Lee et al. [17] for the following dynamical processes: (i) 1:3 transient resonance capture in a coupled oscillator with essential stiffness nonlinearity [27]; and (ii) triggering mechanism of aeroelastic instability in a rigid wing in flow [28]. In this section, we apply the proposed nonlinear system identification to construct nonlinear interaction models (NIMs) of these two systems. At this point we mention that NIMs are not necessarily reduced order models (ROMs) of the dynamics. The reason is that the dimensionality of NIMs coincides with the number of dominant harmonics participating in the nonlinear modal interactions under consideration; in certain cases (such as in the dynamical processes considered herein), the dimensionality of the NIMs might be greater than the dimensionality of the original dynamical systems generating the dynamics, since the number of dominant harmonics participating in the dynamics might be greater than the number of degrees of freedom of the dynamical system. This is especially true in strongly nonlinear dynamics where a number of fundamental, subharmonic or combination harmonics might significantly affect the evolutions and bifurcations of the dynamical processes. In cases, however, where the dimensionality of the original dynamical systems is large (*e.g.*, finite element models of fluid-structure interaction systems, or large-scale structural systems) the identified NIMs will indeed be ROMs of the dynamics, capturing the important dynamics in reduced low-dimensional phase spaces.

4.1 Dynamics of 1:3 transient resonance capture in a coupled oscillator

As a first example, we consider a linear oscillator (LO) coupled to a nonlinear oscillator through an essential stiffness nonlinearity of the third degree. In previous work the nonlinear oscillator was termed a nonlinear energy sink (NES) due to its capacity to passively absorb and locally dissipate energy from the LO over broad frequency ranges [20]. In this section we focus on performing the NSI to study the dynamics of 1:3 transient resonance capture (TRC) between the NES and the LO, assuming no *a priori* system information and performing direct analysis of the time series. The details of the dynamics of this system and the equivalence between the analytical and empirical slow flows can be found in Kerschen et al. [27] and Lee et al. [17], respectively.

For the time series depicted in Fig. 1, Fourier transform (FT) and wavelet transform (WT) spectra show that the response of the LO, $y(t)$, possesses a dominant frequency at $\omega_2 = 0.16$ Hz (or $\omega_2 \approx \omega_0 = 1$ rad/s, where ω_0 is the linearized natural frequency of the LO), whereas that of the NES, $v(t)$, a major harmonic component at $\omega_1 = 0.053$ Hz (or $\omega_1 \approx \omega_2/3$ rad/s) and a minor component at ω_2. We denote the ω_1- and

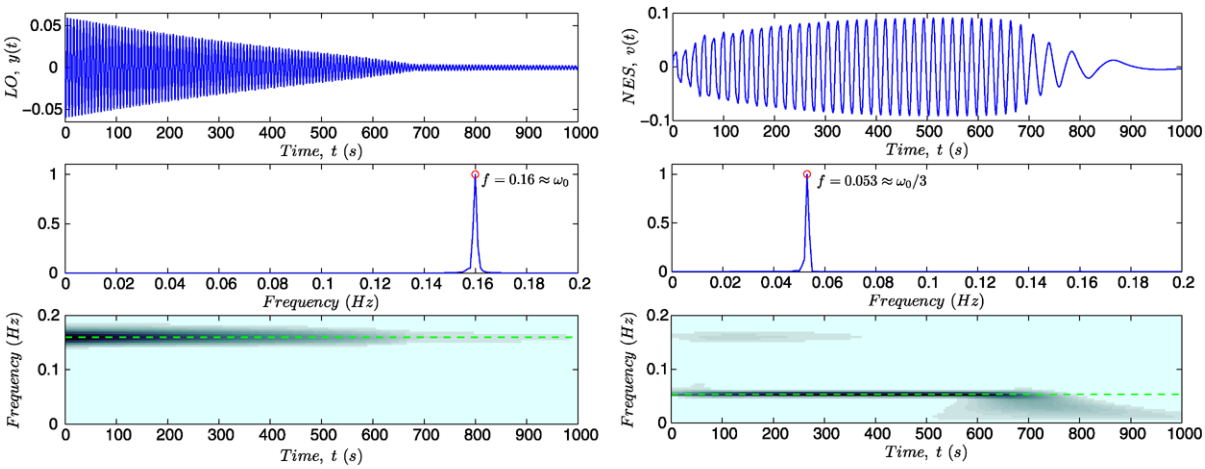

Fig. 1 Frequency components of the numerical responses during 1:3 TRC: (**a**) LO displacement, $y(t)$; (**b**) NES displacement, $v(t)$ [17]

ω_2-components by LF (low-frequency) and HF (high-frequency) components, respectively.

When advanced EMD (AEMD [17]) analysis of the time series is performed, we obtain the dominant IMFs depicted in Fig. 2. Neglecting the spurious component (*i.e.*, LF LO $c_1^{(1)}(t)$), the resulting decompositions are expressed, respectively, as

$$\begin{aligned} x_1(t) &\triangleq y(t) \approx c_2^{(1)}(t) \\ x_2(t) &\triangleq v(t) \approx c_1^{(2)}(t) + c_2^{(2)}(t) \end{aligned} \tag{45}$$

where super- and subscripts of the IMFs indicate the orders of the system (DOF) and frequency components, respectively. Compatible with the WT spectra of the respective decompositions, the IMFs are well-separated or 'proper' [17].

Based on these results we construct a NIM describing the strongly nonlinear interaction (1:3 resonance capture) between the LO and the NES in the form of a set of uncoupled but forced IMOs

$$\begin{aligned} &\text{HF LO}: \ddot{x}_1^{(2)}(t) + 2\zeta_1^{(2)}\omega_2\dot{x}_1^{(2)}(t) + \omega_2^2 x_1^{(2)}(t) \\ &\qquad \approx \mathrm{Re}[\Lambda_1^{(2)}(t)e^{j\omega_2 t}] \\ &\text{LF NES}: \ddot{x}_2^{(1)}(t) + 2\zeta_2^{(1)}\omega_1\dot{x}_2^{(1)}(t) + \omega_1^2 x_2^{(1)}(t) \\ &\qquad \approx \mathrm{Re}[\Lambda_2^{(1)}(t)e^{j\omega_1 t}] \\ &\text{HF NES}: \ddot{x}_2^{(2)}(t) + 2\zeta_2^{(2)}\omega_2\dot{x}_2^{(2)}(t) + \omega_2^2 x_2^{(2)}(t) \\ &\qquad \approx \mathrm{Re}[\Lambda_2^{(2)}(t)e^{j\omega_2 t}] \end{aligned} \tag{46}$$

The forcing terms are in the form of 'fast' oscillating terms $e^{j\omega_m t}$, $m = 1, 2$, modulated by the 'slowly-varying' complex amplitudes $\Lambda_k^{(m)}(t)$, $k = 1, 2$, which implies that the forcing amplitudes $\Lambda_k^{(m)}(t)$ vary much slower than the corresponding carrying signals $e^{j\omega_m t}$.

As discussed in Sect. 3, the main motivation for constructing the NIM (46) is that the response of the respective IMOs approximately reproduces the corresponding dominant IMF of the time series of the 1:3 TRC between the NES and the LO. Since the superposition of the IMFs reconstructs the original time series (*cf.* Lee et al. [17]), the same should hold for the combined response of the IMOs in (46); that is, the synthesis of the IMOs should reproduce the original time series, $y(t) \approx x_1^{(2)}(t)$ and $v(t) \approx x_2^{(1)}(t) + x_2^{(2)}(t)$. The reasoning behind the specific structure of the IMOs (46) (*i.e.*, in the form of a set of linear damped and forced oscillators) lies in the fact that each of the dominant IMFs of the LO and the NES responses possesses two constant fast frequencies approximately equal to the linearized natural frequency of the LO (*i.e.*, $\omega_2 = \omega_0$) and one third of it (*i.e.*, $\omega_1 = \omega_0/3$), respectively. It follows that, at least in principle, each of the dominant IMFs can be regarded as the response of the damped linear oscillator (*i.e.*, an IMO) with a natural frequency equal to either one of the two dominant frequencies ω_0 and $\omega_0/3$, and linear viscous damping factors $\zeta_k^{(m)}$, $k, m = 1, 2$.

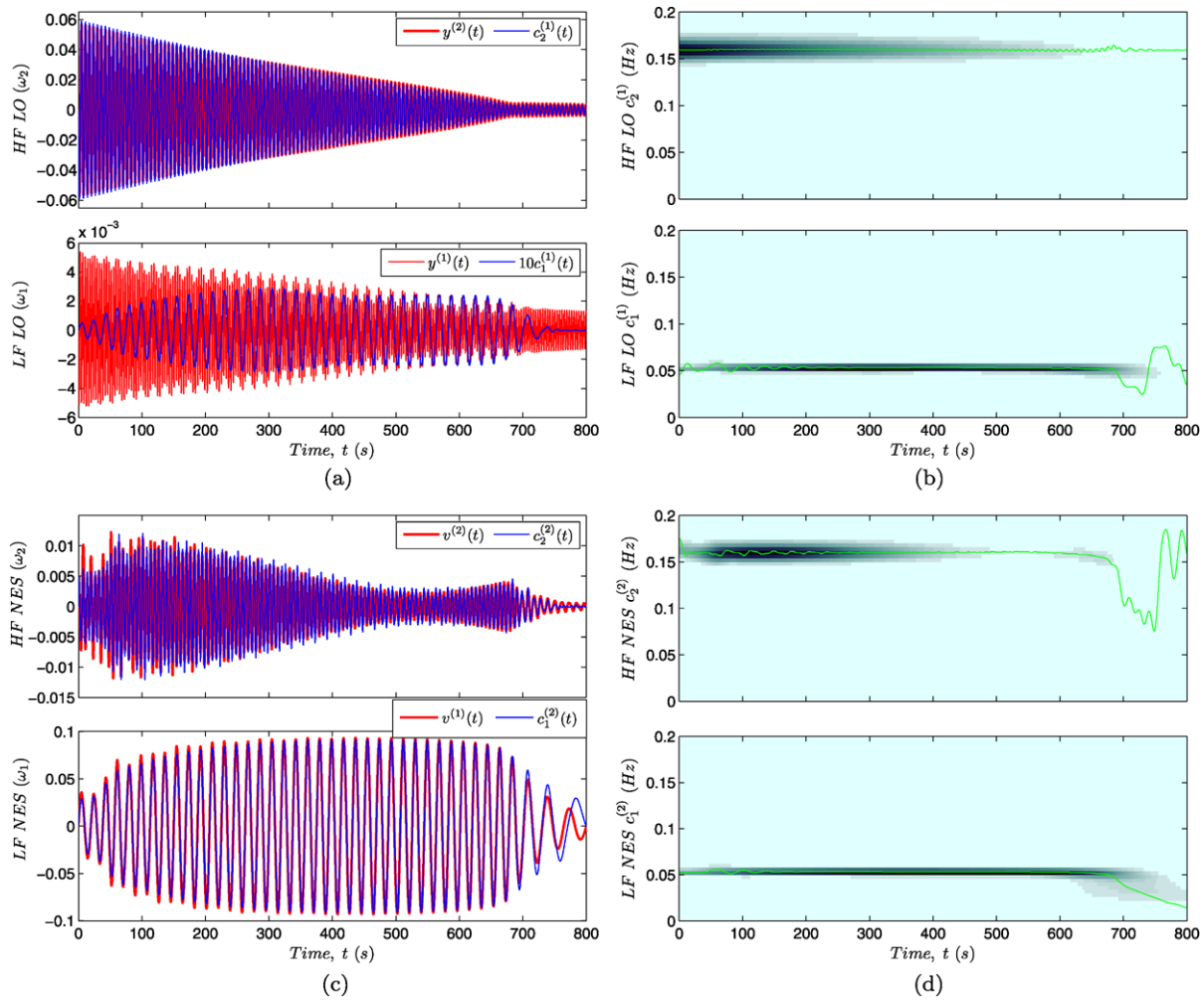

Fig. 2 Comparison of respective frequency components of displacements derived from the analytical slow flow and the IMFs, (**a**) for the LO, and (**c**) for the NES; the wavelet spectra of the corresponding IMFs are depicted in (**b**) and (**d**), respectively; the instantaneous frequencies of the IMFs are superimposed to the wavelet spectra [17]

Also, we note that the forcing terms in (46) are approximated as modulated periodic signals with fast frequencies equal to the eigenfrequencies of the IMOs. The rationale for this is that any excitations possessing frequencies other than the ones selected will be off-resonance and, therefore, their contributions to the resulting dynamics would be less significant, of a secondary nature. In essence, these forcing terms represent the nonlinear modal interactions between the LO and the NES occurring at the dominant fast frequencies of the dynamics (*cf.* Sect. 3).

Computation of the amplitudes of the nonlinear modal interactions in (46) is performed in three ways as described in Sect. 3. Since the analytical slow flow resulting from CX-A analysis has been performed already for this system [27], we may employ it for directly estimating the nonlinear modal interactions through expressions similar to (30). Alternatively, we may utilize the numerical IMFs and estimate the amplitudes of the nonlinear modal interactions by means of relation (32) or its simplified form (34). Hence, we will use three alternative ways to estimate the forcing terms in the NIM (46), all of which will be employed in the following numerical computations. We reiterate at this point that when no slow-flow model of the dynamics is known (*e.g.*, in cases where we consider experimentally obtained time series) we can only utilize expressions (30) or (34) to estimate the amplitudes of

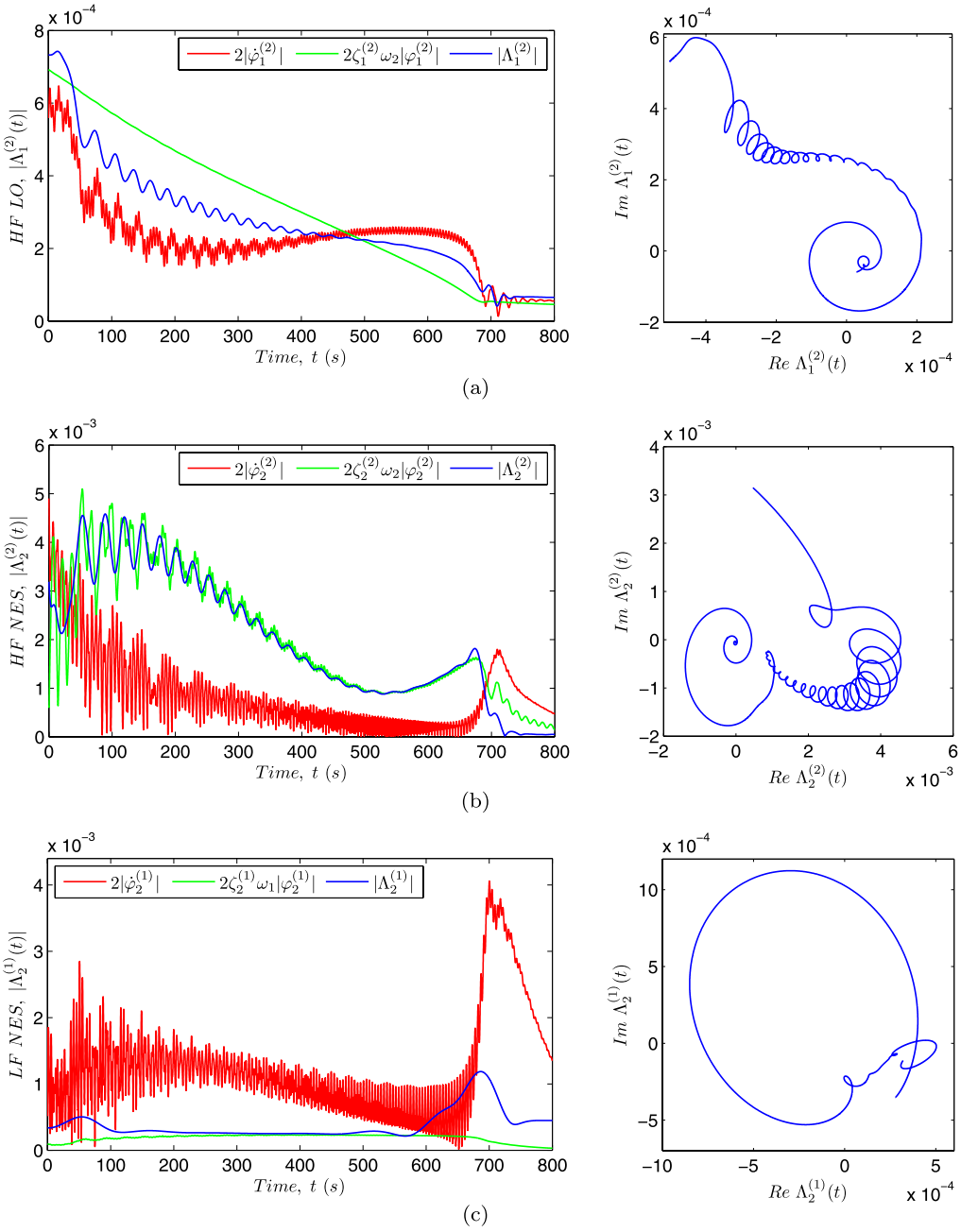

Fig. 3 Nonlinear modal interactions (30) computed from the analytical slow flow: (**a**) HF LO ($\zeta_1^{(2)} = 0.006$); (**b**) HF NES ($\zeta_2^{(2)} = 0.2$); (**c**) LF NES ($\zeta_2^{(1)} = 0.011$)

the nonlinear modal interactions by means of the numerically derived IMFs (instead of the more accurate analytically-based expression (46)).

Figure 3 depicts the computation of the amplitudes of the nonlinear modal interactions using the analytical slow flow derived through CX-A (expression (30)). Superimposed on these plots are the magnitudes $2|\dot{\varphi}_k^{(m)}(t)|$ and $|2\zeta_k^{(m)}\omega_m\varphi_k^{(m)}(t)|$ in order to check which term significantly contributes to the amplitudes of the nonlinear modal interactions $|\Lambda_k^{(m)}(t)|$

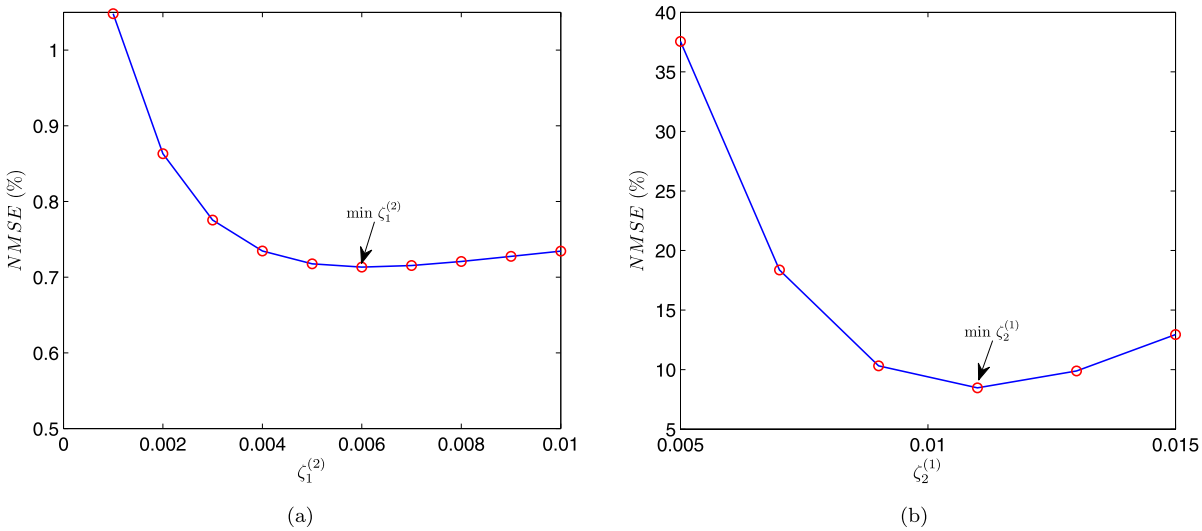

Fig. 4 Computation of normalized mean square errors (NMSEs, %) to determine optimal damping factors for (**a**) HF LO; (**b**) LF NES

(*cf.* relation (30)). We note that low-pass filtering was used in the computation of the amplitudes depicted in Fig. 3 in order to remove high-frequency content and other numerical artifacts from the dynamics. We also note that, except for the HF LO, the amplitudes of the nonlinear modal interactions coincide with the magnitudes of $|2\zeta_k^{(m)}\omega_m\varphi_k^{(m)}(t)|$ while the LO and the NES are engaged in 1:3 TRC (*i.e.*, for $t \lesssim 650$). From this observation, we conjecture that the contribution from the time derivative of the slow flow to the resulting dynamics is negligible, although its effect should not be neglected when interpreting nonlinear modal interactions (*cf.* Sect. 3). We will verify this conjecture by considering the IMO solutions in Fig. 6, and reconstructing the original solutions in Fig. 9.

The damping factors $\zeta_k^{(m)}$ employed in the computations of the nonlinear modal interactions of Fig. 3 were determined by computing the minimum normalized mean square errors (NMSEs) between the envelopes of the dominant IMFs and the corresponding IMO solutions. The formula for computing the NMSEs is

$$\text{NMSE} = \frac{\text{E}[\| \hat{A}_m^{(k)}(t) - \tilde{A}_m^{(k)}(t) \|^2]}{\text{E}[\| \hat{A}_m^{(k)}(t) - \text{E}[\hat{A}_m^{(k)}(t)] \|^2]} \tag{47}$$

where $\text{E}[\cdot]$ implies the expected or mean value; $\|\cdot\|$, the norm between two vectors; $\hat{A}_m^{(k)}(t)$, the envelope of the dominant IMF $c_m^{(k)}(t)$; and $\tilde{A}_m^{(k)}(t)$, the envelope of the corresponding IMO solution $x_k^{(m)}(t)$. These envelopes can be computed by complexification through the application of the Hilbert transform. The time interval for the NMSE computation is taken as $t \in [0.2t_f,\ 0.7t_f]$, where t_f is the end time of the window under consideration. The reason for this is to minimize contamination of the NMSE resulting from end effects (*i.e.*, from EMD). We note that this optimization problem is not set for pointwise match (*i.e.*, in the fast time scale), but rather for pursuing 'global' match (*i.e.*, in the slow time scale) between $c_m^{(k)}(t)$ and $x_k^{(m)}(t)$. Figure 4 presents computational results determining the optimal damping factors for the HF LO and LF NES components. In some cases when the NMSEs decrease gradually but slowly as the damping factor increases, one may select as an acceptable damping value the one corresponding to significant drop of the NMSEs to a sufficiently low value.

We now consider alternative computations of the nonlinear modal interactions based solely on the results of EMD (*i.e.*, on the IMFs). To this end, we compute the amplitudes of the nonlinear modal interactions by means of relation (32) or its simplified form (34). These results are compared in Fig. 5. Both results exhibit similar trends and their differences are attributed to the contribution of the first term (*i.e.*, the time derivative in the slow flow) in (32). Also, comparing the orbits of the respective frequency components in the complex plane in Fig. 5 to those in Fig. 3,

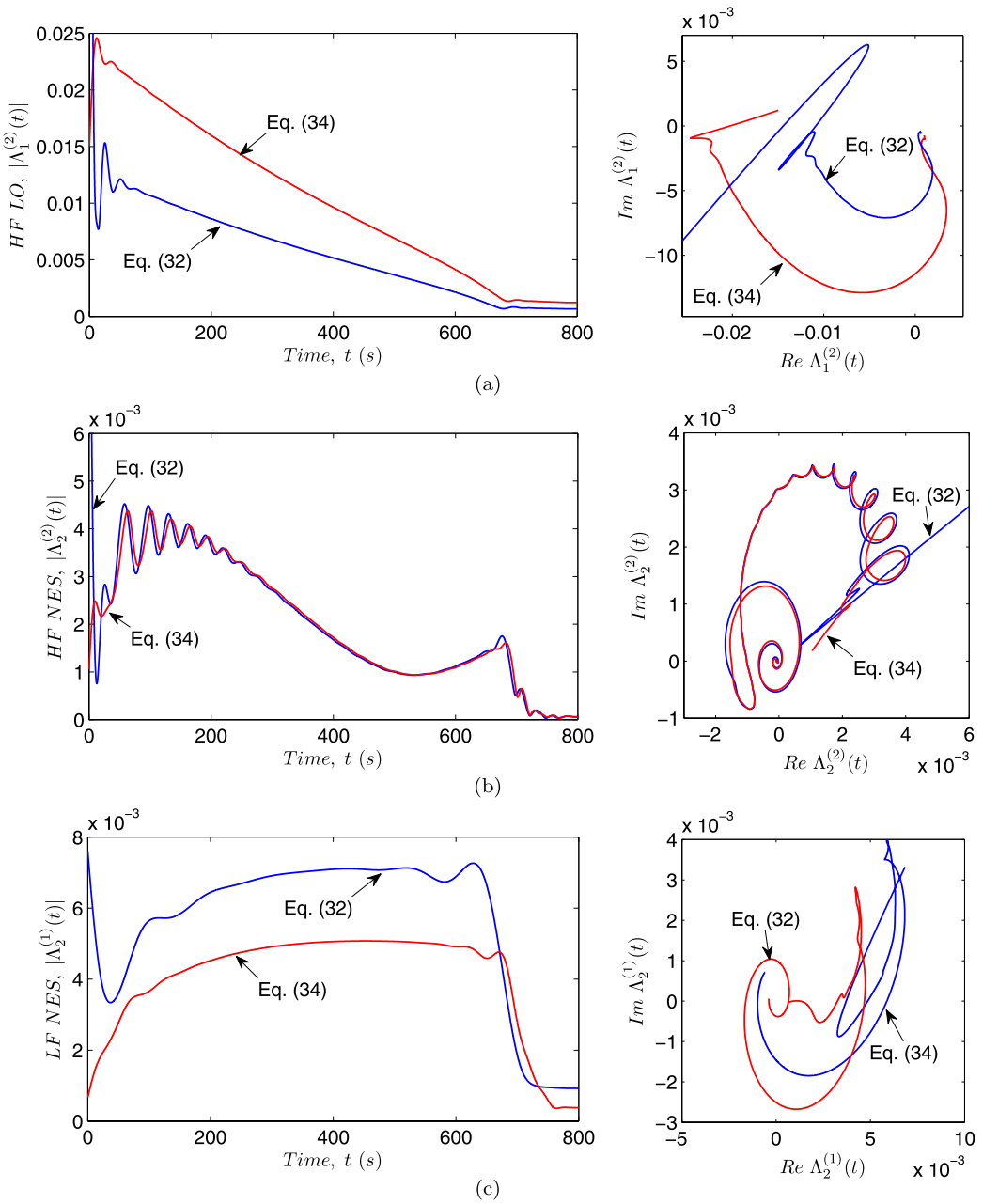

Fig. 5 Nonlinear modal interactions (30) computed from the slow parts of the IMFs using (32) and (34) for, (**a**) the HF LO component ($\zeta_1^{(2)} = 0.11;\ 0.2$); (**b**) the HF NES component ($\zeta_2^{(2)} = 0.2;\ 0.2$); (**c**) the LF NES component ($\zeta_2^{(1)} = 0.35;\ 0.25$)

we find similarity between them; that is, multiplied by $j\omega_m$, the orbits in Fig. 5 coincide approximately with those in Fig. 3. This demonstrates the equivalence relation (19) and validates our premise that the EMD results indeed correspond to the underlying slow dynamics of the system.

We note that the (optimal) damping factors used for computing the previous nonlinear modal interactions are not unique, consistent with the fact that, in general, nonlinear system identification methods result in non-unique models of the dynamical phenomena of interest. The validity of the NIMs (46) identi-

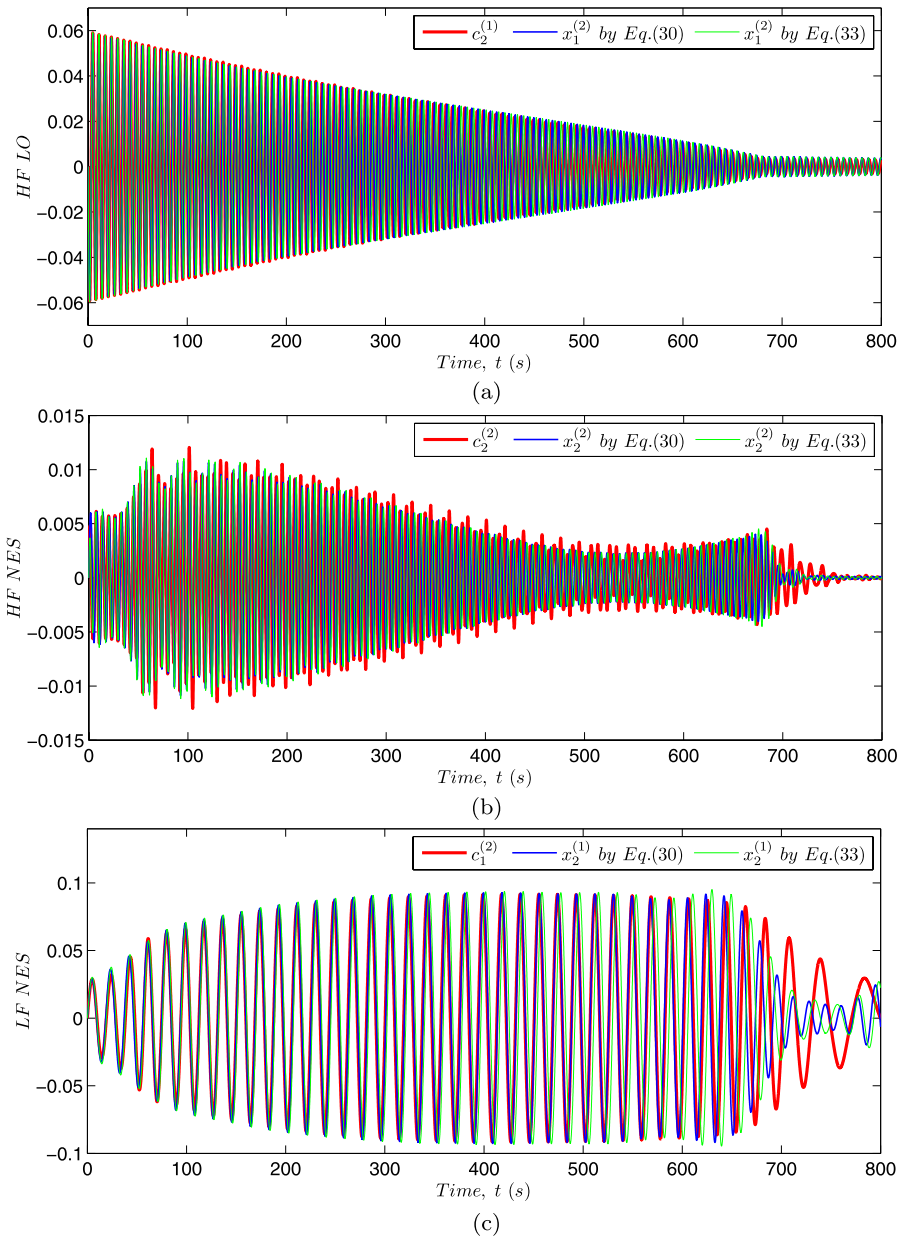

Fig. 6 Responses of the NIM (46) using formula (30) for computing the nonlinear modal interactions from the analytical slow flows, and comparisons with the corresponding IMFs for, (**a**) HF LO; (**b**) HF NES; (**c**) LF NES; the exact solutions by (33) are superimposed to these results

fied previously can be checked by comparing the solutions of the IMOs and their corresponding dominant IMFs. In addition, the accuracy of the proposed NSI method can be verified by checking if the relations

$$y(t) \approx x_1^{(2)}(t) \quad \text{and} \quad v(t) \approx x_2^{(1)}(t) + x_2^{(2)}(t) \qquad (48)$$

are satisfied; that is, if the synthesis of the IMOs accurately reproduces the original time series. Figures 6–8 compare the IMO solutions to the corresponding dominant IMFs. As was the case when comparing the analytical approximation to the exact solution, the validity of the IMOs is expected to hold only before escape from the 1:3 TRC occurs (*i.e.*,

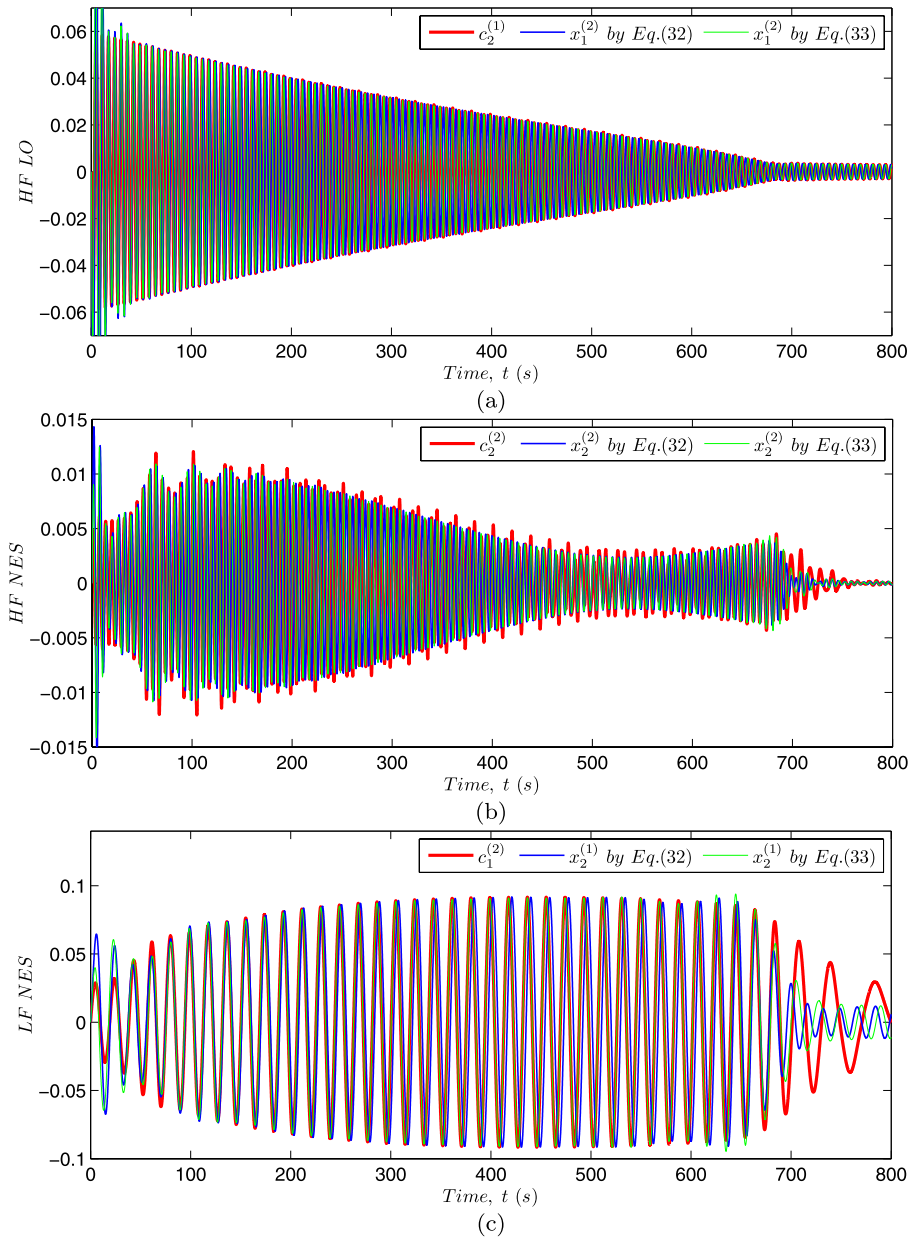

Fig. 7 Responses of the NIM (46) using formula (32) for computing the nonlinear modal interactions, and comparisons with the corresponding IMFs for, (**a**) HF LO; (**b**) HF NES; (**c**) LF NES; the exact solutions by (33) are superimposed to these results

until $t \approx 650$). Moreover, comparing the IMO solutions in Figs. 6 and 8, we may conclude that construction of the nonlinear modal interactions by means of (34) (involving one-step further simplification) will be more useful and time-saving compared with using the more complete expression (32). This observation can also be derived from the comparison of the reconstructed time series (the sum of the IMO solutions) to the original time series (Fig. 9). The IMO solutions and reconstructed time series based on (32) seem to undergo initial overshoots, whereas those based on (34) involve negligible initial undershoots.

4.2 Triggering mechanism of aeroelastic instability

As a second example, we apply the NSI method to studying the triggering mechanism for limit cycle os-

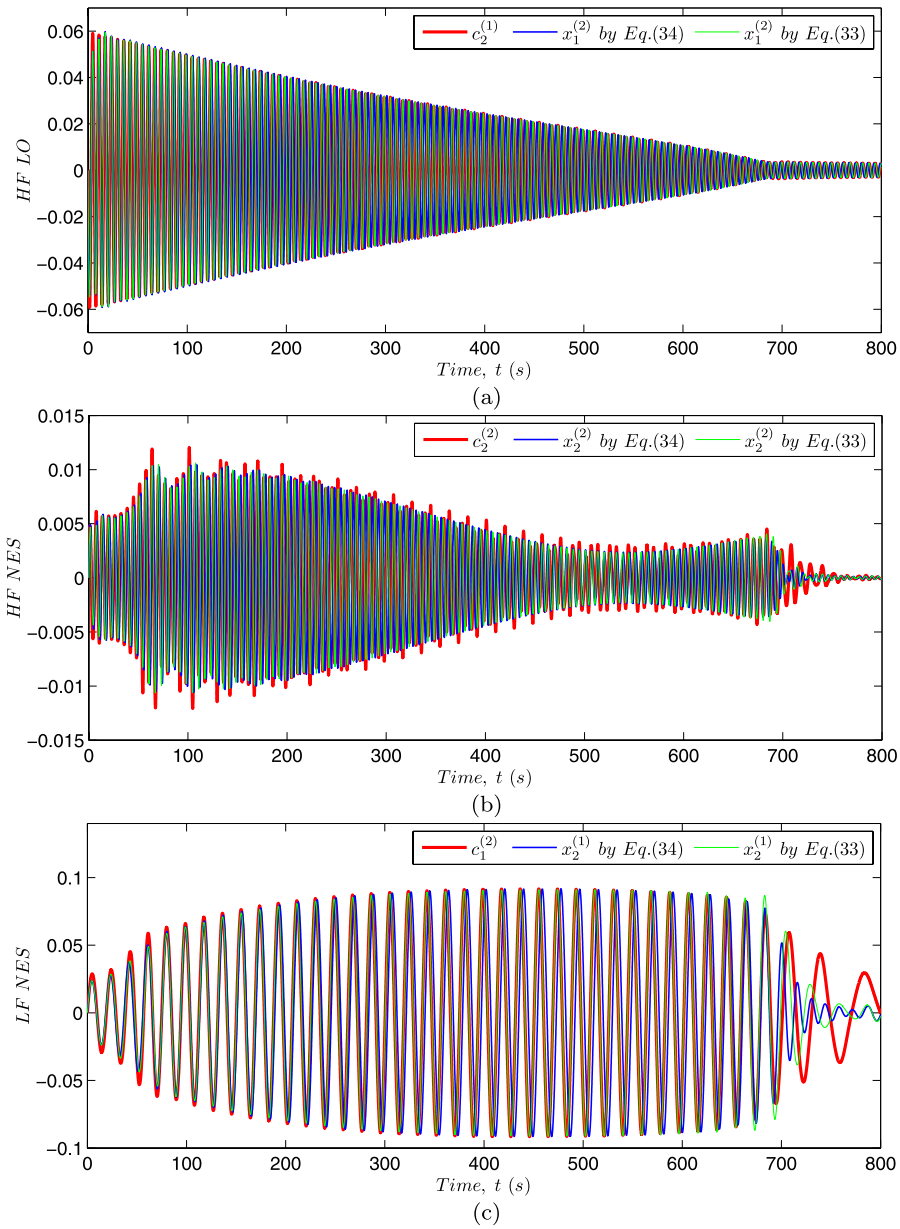

Fig. 8 Responses of the NIM (46) using formula (34) for computing the nonlinear modal interactions, and comparisons with the corresponding IMFs for (**a**) HF LO; (**b**) HF NES; (**c**) LF NES; the exact solutions by (33) are superimposed to these results

cillations (LCOs) of a rigid wing in flow studied in Lee et al. [28]. Analytical study and a demonstration of the equivalence between the analytical and empirical slow flows for this system were performed in Lee et al. [17, 28], respectively. A typical generation of aeroelastic instability in the form of an LCO is depicted in Fig. 10; as discussed in Lee et al. [28] an initial 1:1 transient resonance capture (TRC) between the heave and pitch modes acts as 'trigger' for a 1:3 permanent resonance capture (PRC) between the same modes and gives rise to the LCO. Here we focus only on system identification from the time series depicted in Fig. 10 by presuming no *a priori* system information, except for the fact that $y(t)$ $(\alpha(t))$ is the computational time series of the heave (pitch) mode.

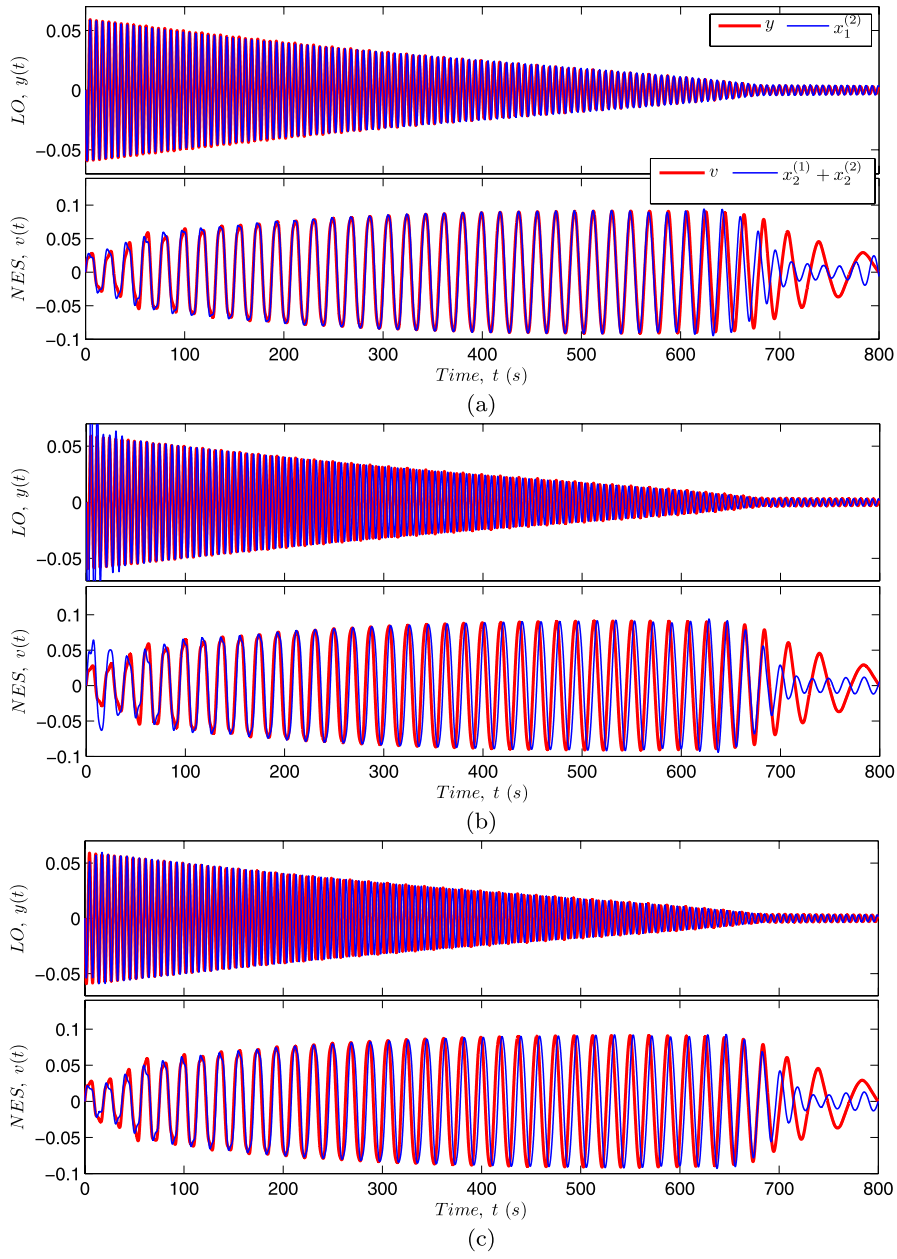

Fig. 9 Reconstruction of the original time series from the NIM (46) when the nonlinear modal interactions are computed by, (**a**) CX-A; (**b**) Equation (32); (**c**) Equation (34)

Referring to the computational results of Fig. 10, the FT and WT spectra show that the heave mode, $y(t)$, possesses two dominant (fast) frequencies at $\omega_1 = 0.135$ Hz (or $\omega_1 \approx \omega_\alpha = 1$ rad/s, where ω_α corresponds to the uncoupled linearized natural frequency of the pitch mode), and at $\omega_2 = 0.453$ Hz (or $\omega_2 \approx 3\omega_\alpha$), whereas the pitch mode, $\alpha(t)$, possesses a single dominant (fast) frequency at $\omega_1 = 0.152 \approx \omega_\alpha$ Hz. We denote the ω_1- and ω_2-components by MF (middle-frequency) and HF (high-frequency), respectively, in order for easy comparison with the previous analytical work in Lee et al. [28]. Since we learned in Lee

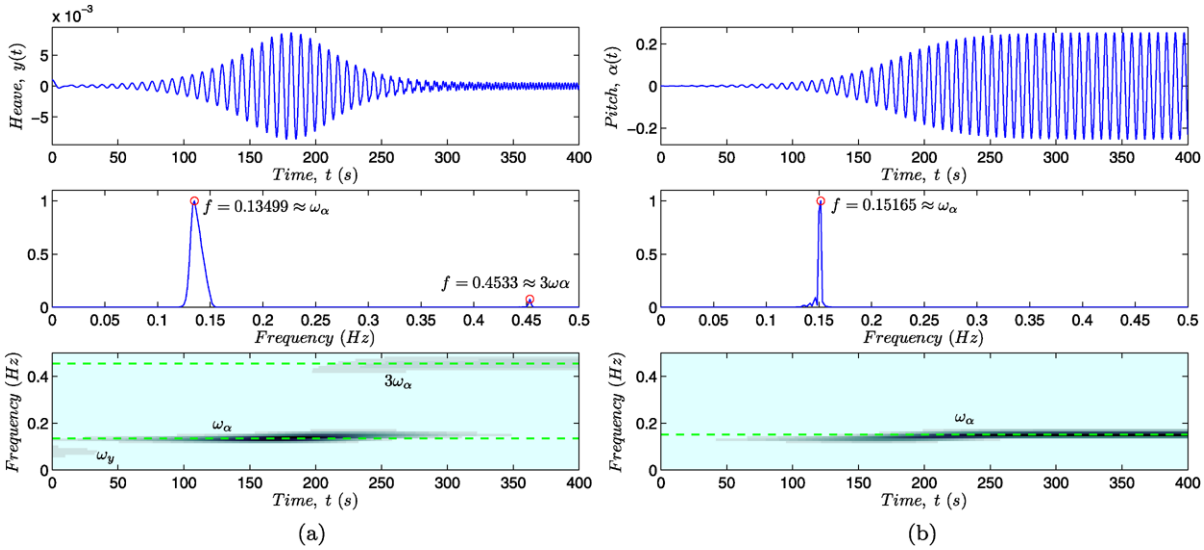

Fig. 10 Frequency components of aeroelastic responses during LCO formation (triggering): (**a**) heave mode $y(t)$; (**b**) pitch mode $\alpha(t)$ [17]

et al. [17] that the choice of proper frequency values can reveal drawbacks in accuracy of the corresponding dominant IMFs, in the following analysis we use the previous frequency values identified from the FT and WT spectra. Note that the frequencies for the MF heave and pitch components are not exactly identical, yet they approximately satisfy a condition of 1:1 resonance during the initial triggering of the LCO.

Considering the results of AEMD analysis of the transient responses depicted in Fig. 11, two dominant IMFs (for the MF and HF components) for the heave mode, and a single dominant IMF (for the MF component) for the pitch mode are identified [17]. Then, the resulting empirical decomposition can be written as

$$\begin{aligned} x_1(t) &\triangleq y(t) \approx c_1^{(1)}(t) + c_2^{(1)}(t) \\ x_2(t) &\triangleq \alpha(t) \approx c_1^{(2)}(t) \end{aligned} \tag{49}$$

Based on our previous discussion, we create a 3-DOF NIM in this case, and write the IMOs reproducing the dominant IMFs as

$$\begin{aligned} &\text{HF heave}: \ddot{x}_1^{(2)}(t) + 2\zeta_1^{(2)}\omega_2\dot{x}_1^{(2)}(t) + \omega_2^2 x_1^{(2)}(t) \\ &\qquad \approx \mathrm{Re}[\Lambda_1^{(2)}(t)e^{j\omega_2 t}] \\ &\text{MF heave}: \ddot{x}_1^{(1)}(t) + 2\zeta_1^{(1)}\omega_1\dot{x}_1^{(1)}(t) + \omega_1^2 x_1^{(1)}(t) \\ &\qquad \approx \mathrm{Re}[\Lambda_1^{(1)}(t)e^{j\omega_1 t}] \end{aligned} \tag{50}$$

$$\begin{aligned} &\text{MF pitch}: \ddot{x}_2^{(1)}(t) + 2\zeta_2^{(1)}\omega_1\dot{x}_2^{(1)}(t) + \omega_1^2 x_2^{(1)}(t) \\ &\qquad \approx \mathrm{Re}[\Lambda_2^{(1)}(t)e^{j\omega_2 t}] \end{aligned}$$

The next step is to compute the nonlinear modal interactions for respective IMOs (*cf.* Fig. 12); in this case we compute these interactions directly from the numerical IMFs utilizing the approximate formula (34). The validity of the results is checked by comparing the IMO solutions to the respective IMFs in Fig. 13; in addition, the IMOs are validated by comparing the reconstructed time series resulting from synthesis of the IMO solutions with the original time series (*cf.* Fig. 14). Except for the initial overshoot in the MF pitch component (and thus in the reconstructed pitch mode) and a slight phase mismatch, the reconstructed time series eventually exhibit reasonable match with the original time series, which demonstrates the validity of the derived NIM and the NSI method.

In summary, we modeled the dynamics of interest (1:3 TRC between the LO and the NES; and the transition from 1:1 TRC to 3:1 PRC which constitute the triggering mechanism of aeroelastic instability) in terms of a NIM in the form of a set of uncoupled but forced IMOs, and demonstrated validity of the IMOs by comparing the reconstructed and original time series. In doing so, it was presumed that there is no *a priori* information about the system (such as masses, spring characteristics, and so

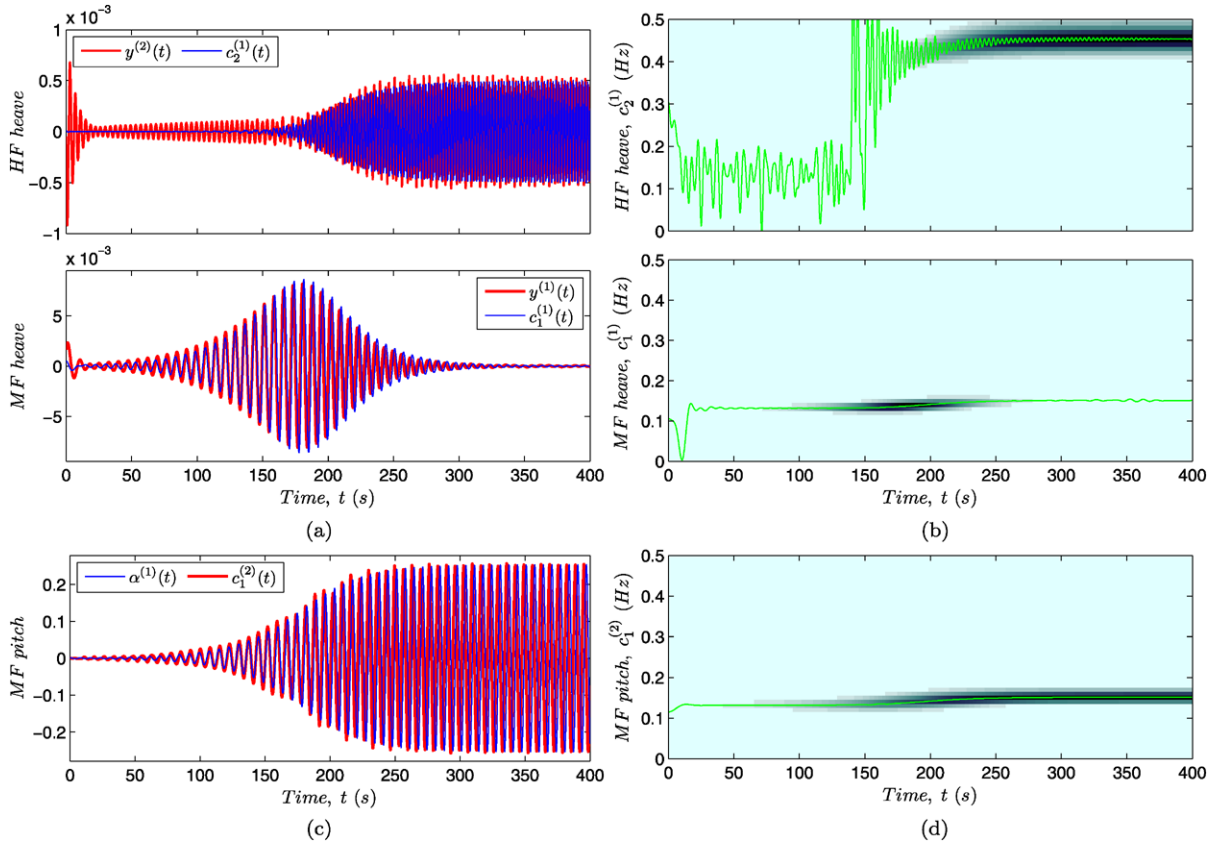

Fig. 11 Comparison of respective frequency components of displacements derived from the analytical slow flow and the IMFs, (**a**) for the heave mode, and (**c**) for the pitch mode; the wavelet spectra of the corresponding IMFs are depicted in (**b**) and (**d**), respectively; the instantaneous frequencies of the IMFs are superimposed to the wavelet spectra [17]

on), since the system identification was based only on the numerical post-processing of the original time series.

5 Concluding remarks

Based on the correspondence between the analytical and empirical slow-flow analyses [17], we developed a time-domain nonlinear system identification (NSI) technique. This NSI method is based on direct analysis of measured time series, and is capable of analyzing strongly nonlinear, complex, multi-component systems. For this purpose, we established expressions for intrinsic mode oscillators (IMOs), which are defined as *the linear equivalent oscillators that can reproduce a given time series at different time scales*. For proper empirical slow-flow decompositions, IMOs are typically expressed as a set of linear, damped oscillators with nonhomogeneous terms providing the nonlinear modal interactions at the different time scales of the dynamics. Both analytical and empirical slow flows were utilized to calculate the nonlinear modal interactions, which were validated by comparing the IMO solutions and the corresponding intrinsic mode functions obtained from empirical mode decomposition. Finally, the overall validity of the proposed method was demonstrated by comparing the reconstructed time series (as synthesis of IMO solutions) to the original time series. A main advantage of our proposed technique is that it is nonparametric, eliminating the necessity for *a priori* assumption of functional forms for stiffness and damping nonlinearities, which might restrict system identification. Hence, at least in principle, it is applicable to a broad range of

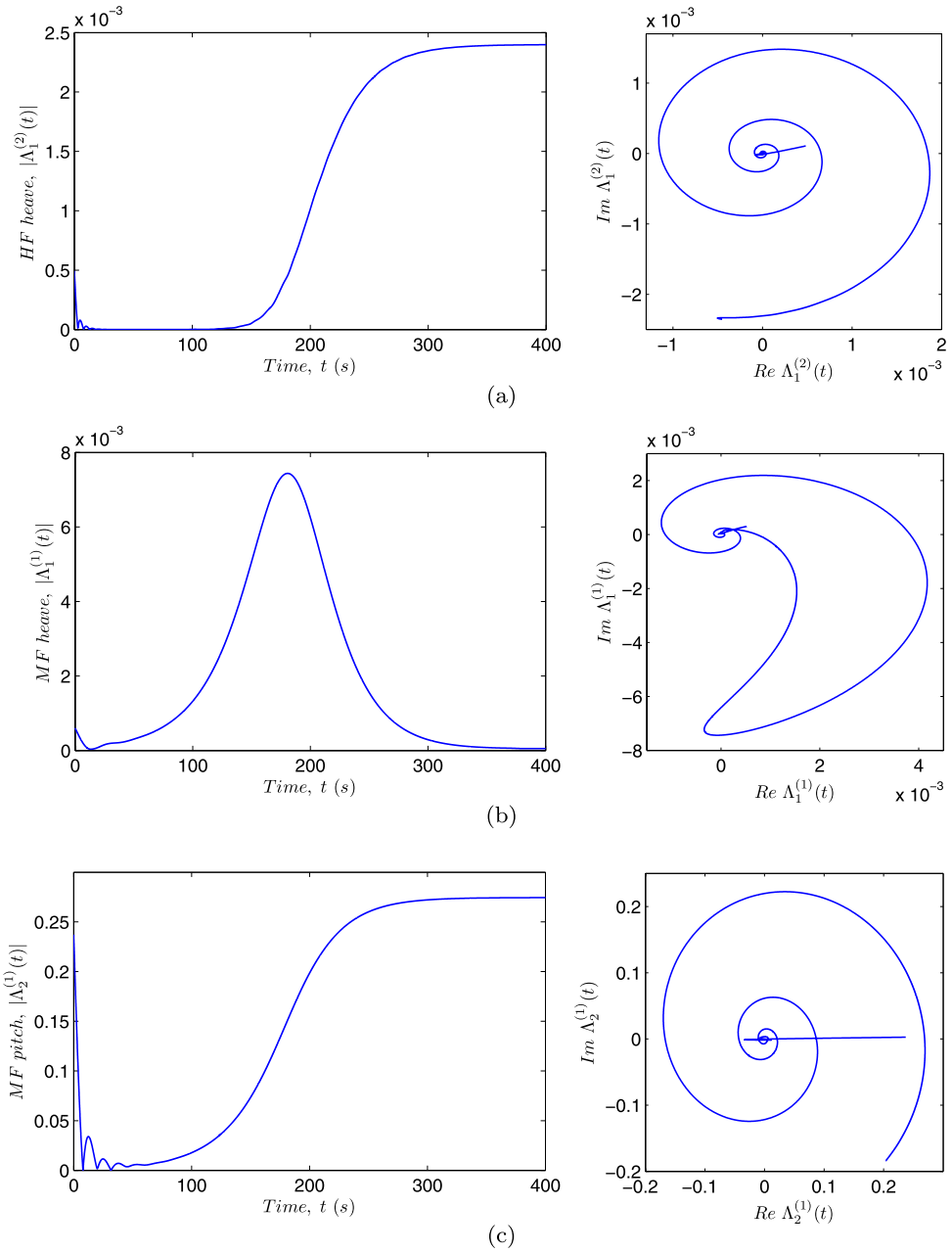

Fig. 12 Nonlinear modal interactions (30) computed from the slow parts of the IMFs using (34), for (**a**) the HF heave component ($\zeta_1^{(2)} = 0.3$); (**b**) the MF heave component ($\zeta_1^{(1)} = 0.6$); (**c**) the MF pitch component ($\zeta_2^{(1)} = 0.6$)

linear as well as nonlinear dynamical systems, including systems with smooth or non-smooth nonlinearities (such as clearances, vibroimpacts, and dry friction), and strong (even nonlinearizable) or weak nonlinear effects; this is due to the fact that the proposed method directly analyzes the actual measured time series which contain full information of the dynamics and do not rely on computed characteristics of the signals (such as FT analysis). In addition, it is multi-scale and directly provides a measure of the dimensionality of the underlying dynamics (which can be of much smaller order—indeed, many orders of

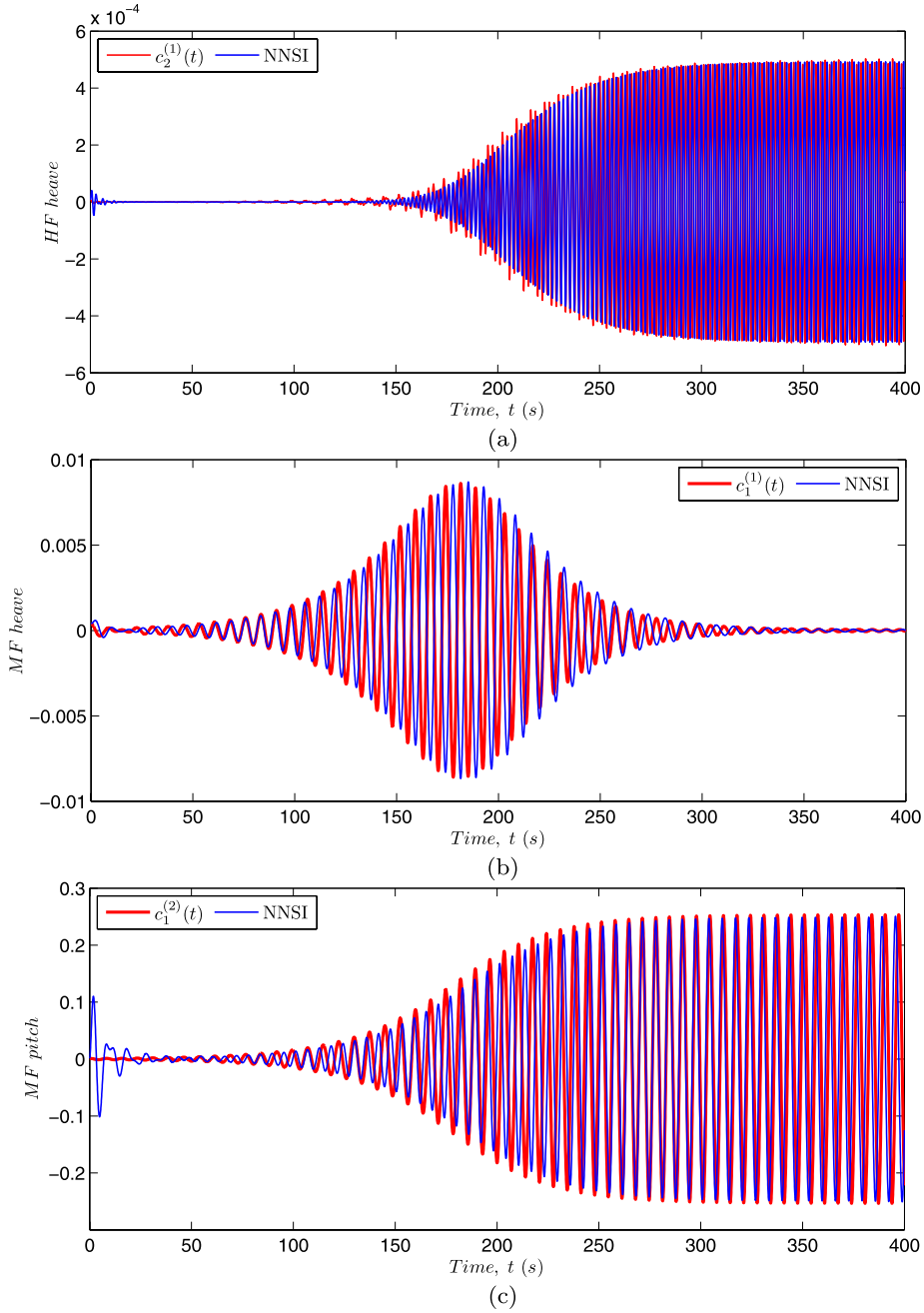

Fig. 13 Responses of the NIM (50) employing (34), and their comparisons with the corresponding IMFs for, (**a**) the HF heave component; (**b**) the MF heave component; (**c**) the MF pitch component

magnitude smaller) than the dimensionality of the underlying computational model. Finally, the method is computationally tractable, conceptually meaningful, and can be used for the construction of accurate low-order models of the dynamics that fully capture the basic resonant interactions between components that give rise to complex and rich dynamical phenomena, such as sudden nonlinear transitions, formation of instabilities, and multi-frequency behavior.

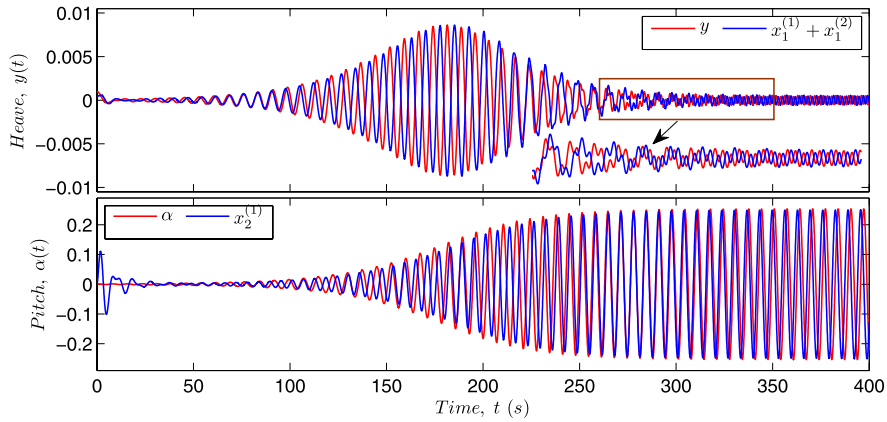

Fig. 14 Reconstruction of the original time series from the NIM (50)

References

1. Ewins DJ (1990) Modal testing: theory and practice. Research Studies Press, Baldock
2. Ibrahim SR, Mikulcik EC (1973) A time domain modal vibration test technique. Shock Vib Bull 43:21–37
3. Juang J-N, Pappa R (1985) An eigensystem realization algorithm for modal parameter identification and model reduction. J Guid Control Dyn 8(5):620–627
4. Van Overschee P, De Moor B (1995) A unifying theorem for three subspace system identification algorithms. Automatica 31(12):1853–1864
5. Kerschen G, Worden K, Vakakis AF, Golinval J-C (2006) Past, present and future of nonlinear system identification in structural dynamics. Mech Syst Signal Process 20(3):505–592
6. Silva W (2005) Identification of nonlinear aeroelastic systems based on the Volterra theory: Progress and opportunities. Nonlinear Dyn 39(1):25–62
7. Masri S, Caughey T (1979) A nonparametric identification technique for nonlinear dynamic systems. Trans ASME J Appl Mech 46:433–441
8. Leontaritis IJ, Billings SA (1985) Input-output parametric models for nonlinear systems. Part I. Deterministic nonlinear systems. Int J Control 41:303–328
9. Leontaritis IJ, Billings SA (1985) Input-output parametric models for nonlinear systems. Part II. Stochastic nonlinear systems. Int J Control 41:329–344
10. Feldman M (1994) Non-linear system vibration analysis using Hilbert transform—I. Free vibration analysis method 'Freevib'. Mech Syst Signal Process 8(2):119–127
11. Feldman M (1994) Non-linear system vibration analysis using Hilbert transform—II. Forced vibration analysis method 'Forcevib'. Mech Syst Signal Process 8(3):309–318
12. Thothadri M, Casas RA, Moon FC, D'Andrea R, Johnson CR (2003) Nonlinear system identification of multi-degree-of-freedom systems. Nonlinear Dyn 32(3):307–322
13. Masri S, Miller R, Saud A, Caughey T (1987) Identification of nonlinear vibrating structures. I. Formulation. Trans ASME J Appl Mech 54(4):918–922
14. Masri S, Miller R, Saud A, Caughey T (1987) Identification of nonlinear vibrating structures. II. Applications. Trans ASME J Appl Mech 54(4):923–950
15. Masri SF, Caffrey JP, Caughey TK, Smyth AW, Chassiakos AG (2005) A general data-based approach for developing reduced-order models of nonlinear MDOF systems. Nonlinear Dyn 39(1):95–112
16. Masri S, Tasbihgoo F, Caffrey J (2007) Development of data-based model-free representation of non-conservative dissipative systems. Int J Non-Linear Mech 42(1):99–117
17. Lee YS, Tsakirtzis S, Vakakis AF, Bergman LA, McFarland DM (2009) Physics-based foundation for empirical mode decomposition. AIAA J 47(12):2938–2963. doi:10.2514/1.43207
18. Manevitch LI (1999) Complex representation of dynamics of coupled nonlinear oscillators. In: Mathematical models of non-linear excitations, transfer, dynamics, and control in condensed systems and other media, pp 269–300
19. Manevitch LI (2001) The description of localized normal modes in a chain of nonlinear coupled oscillators using complex variables. Nonlinear Dyn 25:95–109
20. Vakakis AF, Gendelman O, Bergman LA, McFarland DM, Kerschen G, Lee YS (2008) Passive nonlinear targeted energy transfer in mechanical and structural systems: I and II. Springer, Berlin
21. Lochak P, Meunier C (1988) Multiphase averaging for classical systems: with applications to adiabatic theorems. Springer, Berlin
22. Huang N, Shen Z, Long S, Wu M, Shih H, Zheng Q, Yen N-C, Tung C, Liu H (1998) The empirical mode decomposition and the Hilbert spectrum for nonlinear and non-stationary time series analysis. Proc R Soc Lond, Ser A Math Phys Sci 454:903–995
23. Rilling G, Flandrin P, Gonçalvès P (2003) On empirical mode decomposition and its algorithms. In: IEEE-Eurasip workshop on nonlinear signal and image processing, Grado, Italy
24. Sharpley RC, Vatchev V (2004) Analysis of the intrinsic mode functions. Industrial Mathematics Institute (IMI) Technical Reports, Department of Mathematics, University of South Carolina, No 12

25. Nayfeh A, Mook D (1979) Nonlinear oscillations. Wiley, New York
26. Bedrosian E (1963) A product theorem for Hilbert transform. Proc IEEE 51:868–869
27. Kerschen G, Lee YS, Vakakis AF, McFarland DM, Bergman LA (2006) Irreversible passive energy transfer in coupled oscillators with essential nonlinearity. SIAM J Appl Math 66(2):648–679
28. Lee YS, Vakakis AF, Bergman LA, McFarland DM, Kerschen G (2005) Triggering mechanisms of limit cycle oscillations due to aeroelastic instability. J Fluids Struct 21(5–7):485–529